

Identifying Latent Intentions via Inverse Reinforcement Learning in Repeated Linear Public Good Games

Carina I. Hausladen¹, Christoph Engel², and Marcel Schubert²

¹ETH Zurich, Computational Social Science

²Max Planck Institute for Research on Collective Goods

Abstract

Behavior in repeated public goods games continues to challenge standard theory: heterogeneous social preferences can explain first-round contributions, but not the substantial volatility observed across repeated interactions. Using 50,390 decisions from 2,938 participants, we introduce two methodological advances to address this gap. First, we cluster behavioral trajectories by their temporal shape using Dynamic Time Warping, yielding distinct and theoretically interpretable behavioral types. Second, we apply a hierarchical inverse Q-learning framework that models decisions as discrete switches between latent cooperative and defective intentions. This approach reveals a large (21.4%) and previously unmodeled behavioral type—Switchers—who frequently reverse intentions rather than commit to stable strategies. At the same time, the framework recovers canonical strategic behaviors such as persistent cooperation and free-riding. Substantively, recognizing intentional volatility helps sustain cooperation: brief defections by Switchers often reverse, so strategic patience can prevent unnecessary breakdowns.

1 Introduction

Cartels owe their fragility to a simple economic fact: cooperation is difficult to sustain when individual incentives point the other way. Economists often model this tension as a repeated public-goods dilemma. This framework is particularly apt for tacit collusion, where firms coordinate without explicit agreements. Here, defection remains individually tempting, but implicit coordination mechanisms—such as delayed punishments or “noisy” attempts to restore discipline can sustain cooperative outcomes [1]. Similar dynamics arise well beyond cartels. Many financial markets are characterised by sequences of interdependent actions: Market-making, for instance, depends on a continuous stream of liquidity provision that is costly to supply yet easily exploited [2]. Banks engage in funding-liquidity management, watch one another’s positions and adjust their own in response [3]. Clearing members in derivatives markets face shared margin obligations, where one firm’s stress can force others to contribute more [4]. These environments, such as public-goods games, produce time series of contributions and withdrawals that are mutually conditioned. The laboratory model thus provides a useful lens for studying their behaviour.

In this context, standard theory predicts the tragedy of the commons. Everybody maximizes individual profit and exploits the socially-minded choices of others. If community members interact repeatedly, but it is known

when interaction will stop, the gloomy prediction still holds [5]. A robust experimental literature shows that, in the aggregate, results look different. In a standard symmetric linear public good game, average contributions typically start considerably above zero, but tend to decline over time [6–12]. A substantial theoretical literature rationalizes this result by introducing some form of social preferences into the utility function [10–13], whereas other scholars attribute cooperation to confusion, arguing that participants misinterpret the game [14–16]. Efforts to disentangle cooperation driven by social preferences from that motivated by confusion have not reached a consensus. A widely accepted view posits that observed contributions stem from a combination of confusion and social preferences [17–19]. Some work argues that social preferences do not account for human cooperation at all, but instead, confusion does [16]. Very recently, this conclusion was challenged [20].

Thus, the question of whether and how social preferences explain cooperative behavior in social dilemma games remains unresolved. This, in particular, holds for the development of contributions over time. Previous research has made important progress by analyzing experimentally generated gameplay data through partitioning approaches that interpret resulting clusters through the lens of established behavioral types. These methods have yielded valuable insights into heterogeneity in social preferences. However, two methodological considerations suggest opportunities for refinement.

Corresponding author: carinah@ethz.ch

First, partitioning typically relies on *pointwise alignment*

ment. While this approach may be suitable for macroeconomic settings where policy changes affect all firms simultaneously, gameplay data tends to exhibit behavioral reactions that are affected by the idiosyncratic experiences in the randomly composed group. We propose using dynamic time warping, a method specifically designed to handle *shifted time series*, for partitioning gameplay data.

Second, the interpretation of partitions has been constrained by strong theoretical priors taken from preference types identified in static settings (e.g., modeling conditional cooperators as participants who match others' cooperation levels). Essentially, this literature *presupposes knowledge of players' reward functions*. Given the persistent presence of unexplainable noise or "other" clusters, we instead argue for explicitly modeling *reward functions as an estimation problem*.

2 Literature

Behavioral Types Categorizing human behavior in social dilemma games has long been of interest to the social sciences. For example, Fischbacher et al. [21] introduced the strategy method as a tool to classify individuals' predispositions toward cooperation in linear public good games.¹ This method isolates preferences from the potential influence of learning dynamics or other mechanisms that may emerge during gameplay. Building on this foundational work, several subsequent studies [12, 21, 23–39] have used the strategy method to identify distinct behavioral types in the very same game. A meta-analysis of these studies [40] found that the latter consistently report the existence of three types: free riders (who contribute nothing, 19.2%), conditional cooperators (whose contributions depend on others' behavior, 61.3 %), and triangle cooperators (10.4%).

Other research has also explored the classification of behavior in public good games, but with a focus on repeated interactions in *gameplay* data rather than data obtained through the strategy method [9, 12, 41–43]. Muller et al. [44] compare both approaches and find that gameplay data often aligns with the classifications derived from the strategy method.

Unlike the strategy method, which assumes a fixed decision rule, gameplay data requires modeling evolving strategies and decision noise. Proposed methods to form taxonomies in *gameplay data* from PGGs include Bayesian models [45], finite mixture models [43], clustering techniques [39, 46], Classifier-Lasso (C-Lasso) [47, 48], and Classification and Regression Trees [49].

A critical point of comparison of these different approaches lies in how these papers accommodate behaviors that elude standard theoretical explanations. Resid-

ual groups are termed "confused" [45], "various" [39], "others" [50], or alternatively are captured through random tremble terms [43]. Their size ranges from 18.5 to 32 percent (see Tab. 1).

These labels—confused, various, others—all implicitly frame the residual group as behavior that cannot (yet) be accommodated by existing theories. When the unexplained share is small, it is pragmatically reasonable not to introduce an additional type: with very few observations, there is simply not enough structure to interpret or model it. However, if nearly one-third of participants behave in ways that existing models fail to capture, it seems no longer appropriate to treat this as mere "noise." Instead, it becomes natural to ask whether these behaviors reflect coherent, yet unmodeled, patterns that deserve explicit interpretation.

A key observation shared across all those studies that propose methods to form taxonomies is the identification of a "downward trend" in public good contributions. This terminology inherently frames the data as time-series and, importantly, emphasizes trends over specific temporal locations of features such as peaks, which may vary due to idiosyncratic group dynamics. However, none of the above-cited papers explicitly addresses this temporal misalignment via their identification strategy.

Theory Driven to Data Driven Identification

The above-cited methods can be placed along a spectrum from theory- to data-driven:

At the theory-driven end, finite mixture models are widely used [e.g., 43], where specific behavioral strategies such as free-riding or conditional cooperation are explicitly modeled. Bayesian mixture models [e.g., 45] offer greater flexibility by estimating individual decision parameters through Bayesian inference, which are then clustered to reveal distinct behavioral types. C-Lasso [47, 50] extends this logic by simultaneously estimating and shrinking parameters in a single step. At the data-driven end, unsupervised machine learning methods—such as clustering—identify behavioral patterns directly from the data [39, 46].

Theory-driven methods often impose assumptions about temporal dynamics—for example, that players respond not only to current but also to past group contributions. Such restrictions may limit their ability to capture evolving strategies, which could help explain why several studies report substantial unexplained variation, with residual clusters ranging from 16% to 32% of observations (Tab. 1). Even data-driven approaches face challenges. Despite their flexibility, existing clustering methods often rely on local distance metrics (e.g., Manhattan distance) that cannot account for misaligned or non-synchronous behavioral trajectories (details in App. A).

Returning to the earlier question: Could the combina-

¹The strategy method has also been criticized for risking confusing social preferences with conditional cooperation [22].

Table 1: Behavioral Type Classifications Across Studies

Study	Conditional/Reciprocal Types			Selfish/Strategic Types		Other	
	Near-rational	Strong CC	Weak CC	Own-Max./Gamesmen	Fatalist	Confused/Others	
Houser (2004)	56%	—	—	—	20%	24%	
Bardsley (2007)	—	—	—	Free-riders: 25% ^a	Altruists: 6% ^a	Trembles: 18.5% ^b	
Fallucci (2021) FM ^d	58% (Recip.)	—	—	9% (Gamesmen)	—	32%	
Fallucci (2021) RM ^d	25% (Recip.)	—	—	52% (Gamesmen)	—	22%	
Fallucci (2019)	—	38.8%	18.9%	25.8% (Own-Max.)	—	21.2% ^c	

Notes: All numbers and descriptions are reported directly from the respective cited studies. *Near-rational*: Behave optimally in line with expected utility. *Fatalist*: Fail to update beliefs properly, acting as if actions have no impact. *Confused/Others*: High randomness or residual unclassified types. *Strong Conditional Cooperators (CC)*: Match others' contributions approximately one-for-one. *Weak CC*: Increase contributions less than proportionally to others' contributions. *Own-Maximizers/Gamesmen*: Purely self-interested strategic players, contributing little or nothing unless beneficial. *Reciprocators*: Respond positively to cooperative behavior.

^a Percentages reflect corrected estimations after accounting for trembles.

^b Initial tremble probability, reflecting random decision errors, decreases significantly with experience.

^c Combines unconditional high contributors (4.7%) and residual (16.5%).

^d Fixed matching (FM); Random Matching (RM).

tion of unaddressed temporal misalignment and the reliance on numerous assumptions contribute to the emergence of an “other” cluster? How might we attempt to better understand such “other” clusters? One promising direction lies in examining methods from the learning literature.

Types in Financial Decision Making Work in behavioral finance also relies heavily on time-series data to identify behavioral types. The data contexts range from retail trading histories [51–53], high-frequency order-flow and inventory trajectories [54, 55], to longitudinal portfolio adjustments [56], fund return dynamics [57, 58], and depositor withdrawal sequences during bank runs [59–61]. A wide variety of behavioral types have been documented across these papers—including retail trading styles, high-frequency trading roles, mutual fund strategy types, and depositor responses in runs (see Tab. S.1). However, this literature typically reduces behavioral trajectories to engineered features, summary statistics, or factor loadings. As a result, interesting types of behavioral heterogeneity may remain hidden.

Reinforcement Learning vs. Intention Switching A long-standing question in behavioral game theory is whether reinforcement learning (RL), and specifically Q-learning, adequately describes how people behave in repeated social dilemmas. Early experimental work demonstrated that RL can capture aggregate patterns of play in repeated games such as the Prisoner’s Dilemma [62]. Hybrid models that combine RL with belief updating fit the data more accurately than either pure RL or belief learning alone [63, 64]. At the neural level, dopamine-based reward prediction error signals have been linked to RL processes, suggesting that Q-learning-like updating is plausible as a cognitive mechanism [65]. Recent work continues to apply and extend Q-learning models to repeated social dilemmas, in-

cluding the Prisoner’s Dilemma and public good games [66, 67].

These models primarily focus on how individuals update action values, rather than on the structure of the underlying reward function [62, 63]. Yet specifying a reward function in a social dilemma is inherently complex: experimental and theoretical evidence shows that people incorporate social preferences—such as fairness, reciprocity, and inequality aversion—in addition to monetary payoffs [68, 69]. Moreover, even a high learning rate in an RL model describes continuous adaptation of beliefs and action values; it does not imply discrete switches in the underlying cooperative intention. Thus, while RL captures some aspects of behavioral adjustment in repeated interactions, it does not explain the sharp intention transitions that characterize the switcher type we identify.

Latent Variable Models Defining a comprehensive and suitable reward function poses challenges in complex behavioral tasks [70, 71]. Inverse Reinforcement Learning (IRL) [72, 73] is a popular approach to recover the reward function inductively from the data. IRL has achieved breakthrough successes in robotics [74, 75] and autonomous driving [76, 77] and has recently also become a valuable tool for constructing mathematical models of animal behavior [70, 78, 79]. Traditionally, the animal’s reward function has been modeled as a *smoothly* time-varying linear combination [80]. More recently, it has been suggested that behavior can be represented as a Markov chain characterized by alternating between *discrete* intentions [81]. In that spirit, Zhu et al. [82] propose a novel class of Hierarchical Inverse Q-Learning (HIQL) algorithms, which extend the fixed-reward inverse Q-learning (IQL) framework [76] to solve multi-intention IRL problems. Notably, HIQL achieves substantially better model fits to behavioral data compared to standard IQL, supporting the idea

that accounting for discrete intentions improves the explanatory power of reward-based learning models.

This paper This paper makes several contributions to the study of cooperation and learning in experimental settings. First, we introduce a method for identifying behavioral patterns in gameplay data that accommodates temporal misalignment—matching trajectories without requiring exact synchronization. We benchmark this DTW-based clustering approach against four established techniques: Bayesian modeling, finite mixture models, C-Lasso, and hierarchical clustering. Second, we apply a latent variable model that allows for *discrete transitions* between latent intentions over time. This framework captures established behavioral types (free riders, unconditional cooperators) while providing a principled interpretation of the previously ambiguous “other” cluster as highly exploratory players who systematically switch between strategies.

3 Methods

The code used for this study will be available in a GitHub repository, which will be made public upon acceptance.

3.1 The Linear Public Good Game

In each round of the linear public good game, every player receives an endowment e and decides how much to contribute c_{it} to a shared project. The total contribution is multiplied by a constant factor μ and evenly distributed among all players. Each player’s payoff is $\pi_{it} = e - c_{it} + \mu \sum_{j=1}^I c_{jt}$, where $0 < \mu < 1$ ensures that contributing benefits the group but is individually costly. To describe a player’s social environment, we define the average contribution of the other group members as $\bar{c}_{-i,t} = \frac{1}{I-1} \sum_{j \neq i}^I c_{jt}$, $t = 1, 2, \dots, T$.

3.2 Identifying Behavioral Types

We propose a two-step approach to identify behavioral types. First, we cluster raw contribution trajectories using a global distance metric that measures similarity in temporal dynamics even when key moments (e.g., peaks or drops) occur at different rounds. This step treats the time series as the primitive object and remains fully model-free: it does not assume a specific objective function or imply that participants foresee the entire series when making decisions. Instead, the second step fits a latent-variable model to each cluster to provide behavioral structure by inferring the intention processes that best rationalize the observed patterns.

This approach adopts a finite-mixture perspective in which each trajectory is generated by one of a small

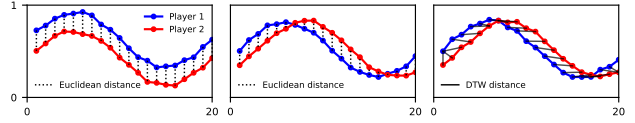


Figure 1: Conceptual Illustration of Euclidean and DTW distances. (Left) Stacked sinusoidal curves represent two players with similar but vertically offset contribution patterns. (Center) Horizontally shifted curves illustrate temporal misalignment between players’ actions; dotted vertical lines denote pairwise Euclidean distances. (Right) DTW alignment paths (black solid lines) show the optimal non-linear correspondence between the two time series, compensating for temporal shifts.

number of latent behavioral types that systematically differ in how they respond over time. Our empirical-first, theory-second strategy follows the spirit of behavioral game theory and applied econometrics, which emphasize data-driven discovery followed by theoretically informed interpretation [83, 84].

3.3 Clustering Multivariate Time-series

Clustering typically involves three steps: (1) selecting the number of clusters, (2) computing pairwise distances between time series, and (3) using these distances to form clusters.

In social dilemma experiments, participants are randomly assigned to groups and thus experience different dynamics—some groups sustain cooperation longer than others. Capturing such variation requires careful choice of the *distance measure* in step (2).

We illustrate the importance of this step using two stylized sinusoidal contribution patterns. In Fig. 1 (left), the two curves are perfectly phase-aligned. In this case, the distance between the two time series can be effectively captured using a local distance metric, such as the point-wise Euclidean distance. However, when the curves are phase-shifted (Fig. 1, middle), the Euclidean distance is no longer an effective similarity measure. Behaviorally, such a phase shift could indicate that two participants are of similar behavioural types but belong to different experimental groups. In this case, a Euclidean comparison fails to group these participants. DTW resolves this limitation by allowing non-linear alignments along the time axis (Fig. 1, right). Instead of comparing points strictly by time index, DTW aligns key structural moments—such as peaks—by warping the time dimension to minimize the overall alignment cost [see 85, for details] (details in App. A).

In addition to time-shifted behavior, social dilemma games have another key feature: they produce *multivariate time series*. In our data, participants play a standard PGG with feedback after each round, showing them the average contribution of their group mem-

bers. Consequently, each participant is associated with two time series: their own contributions, $\{c_{it}\}_{t=1}^T$, and the average contributions of the other group members, $\{\bar{c}_{-i,t}\}_{t=1}^T$. DTW naturally accommodates such multivariate input, allowing us to compare behavioral trajectories across both dimensions (details in App. A).

After computing distances between multivariate time series, a *clustering algorithm* groups the data into meaningful clusters. We evaluate three clustering approaches—partition-based, hierarchical, and graph-based—applied to time series data using DTW as the distance metric. As is standard in unsupervised learning, we compare multiple algorithms and assess their stability and interpretability [86]. Our results show that the specific choice of clustering algorithm has little impact on the resulting cluster structure.

The optimal *number of clusters* k is usually determined using internal cluster validation indices (CVIs). These indices assess clustering quality through different combinations of cluster cohesion and separation metrics [87]. We employ three standard CVIs compatible with DTW-based clustering. We compute their average (normalized) score across candidate cluster numbers (2-20) to select the best number (App. E.1).

To interpret the clusters, it is common to compute a representative time series for each group. While simple averaging is often used, it fails when time series are misaligned. Instead, we use Dynamic Time Warping Barycenter Averaging (DBA) [88], which produces a centroid that preserves the overall shape and timing of behaviors within each cluster. To convey within-cluster heterogeneity, we display interquartile range (IQR) bands at each period.

We assess robustness in three ways. First, we examine sensitivity to modeling choices. While the choice of distance metric has a noticeable impact, different clustering algorithms (given our preferred 2-dimensional DTW metric) yield highly consistent partitions, indicating algorithmic robustness. Second, we evaluate stability using a non-parametric bootstrap. In 100 replications, we resample 80% of individuals, recompute DTW distances, re-estimate spectral clustering, and compare each solution to the baseline using ARI and NMI. This tests how strongly the structure persists under sampling variation. Third, we analyze stability at the individual level. For each subject, we record their cluster assignment across bootstrap replications and compute the share of times they return to their baseline cluster.

3.4 Latent Variable Model

We apply a recently proposed latent variable model that has achieved superior model fit in modeling animal behavior as a Markov chain characterized by alternating between *discrete* intentions. Specifically, this latent variable model is a Hierarchical Inverse Q-Learning (HIQL)

Table 2: Structure of a Q-table.

State	a_1	a_2	a_3
s_1	$Q(s_1, a_1)$	$Q(s_1, a_2)$	$Q(s_1, a_3)$
s_2	$Q(s_2, a_1)$	$Q(s_2, a_2)$	$Q(s_2, a_3)$
s_3	$Q(s_3, a_1)$	$Q(s_3, a_2)$	$Q(s_3, a_3)$

Note: Symbolic Q-values shown for each state-action pair.

algorithm [82].

Q-learning. Q-learning is a fundamental algorithm in RL. The process is typically modeled as a Markov Decision Process (MDP), where the future state s' depends only on the current state s and the chosen action a , formally $P(s' | s, a)$. In the context of the PGG, each player’s *own contribution* can be treated as the *action* $a \in \mathcal{A}$, while the *observed contributions of others* form the *state* $s \in \mathcal{S}$ [67]. Players are assumed to choose actions following an ϵ -greedy policy, balancing exploration and exploitation:

$$a = \begin{cases} \text{a random action,} & \text{with probability } \epsilon, \\ \arg \max_a Q(s, a), & \text{with probability } 1 - \epsilon. \end{cases}$$

Each player maintains a *Q-table* (similar in spirit to Selten’s (1967) Strategy Method, Tab. 2), where rows represent states and columns represent actions, and each entry $Q(s, a)$ encodes the estimated value of taking action a in state s . Initially, the Q-table may contain random or neutral values, but these are updated over time using the standard Q-learning rule:

$$Q_{\text{new}}(s, a) = (1 - \alpha) Q_{\text{old}}(s, a) + \alpha [r + \gamma \max_{a'} Q_{\text{old}}(s', a')] \quad (1)$$

where α is the *learning rate*, controlling how strongly new information replaces old estimates, γ is the *discount factor* that determines the importance of future rewards, and r is the immediate reward received. Under the assumption of perfectly rational agents, the reward function corresponds directly to the payoff function of the PGG. However, empirical evidence suggests that human players exhibit social preferences and bounded rationality, making the reward function difficult to specify explicitly. When this function is treated as unknown and instead inferred from observed behavior, the learning process falls within the class of *Inverse Reinforcement Learning* (IRL).

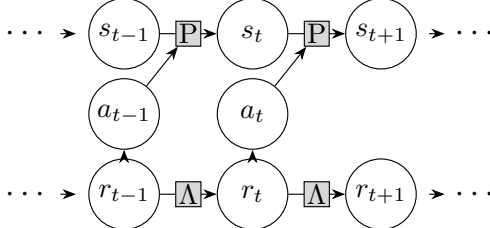
Inverse Q-learning. In *inverse* Q-learning, the situation is reversed: we observe human behavior and aim to infer the underlying reward function that would make such behavior appear optimal. The human is assumed to behave like a Q-learner, but not a perfect one. Given a dataset of observed game trajectories \mathcal{D} , the algorithm

searches for a reward function $r(s, a)$ such that the resulting policy $\pi_r(s, a)$ would most likely have produced the same actions as the human.

Mathematically, this can be expressed as maximizing the likelihood of the observed trajectories under the learned policy: $\max_r \mathbb{E}_{\xi \sim \mathcal{D}} [\log \Pr(\xi | \pi_r)]$, where each trajectory $\xi = \{(s_0, a_0), \dots, (s_n, a_n)\}$ is a sequence of observed state-action pairs. The policy π_r is derived from the learned action-value function $Q(s, a)$, which captures how good each action is in a given state. Inverse Q-learning thus provides a way to *recover the hidden motivations* driving observed decisions, without assuming we already know how people evaluate outcomes (more details in [82, pp 3–5]). The *number of reward functions* r —or latent intentions—is treated as a model parameter and identified empirically through model fit criteria such as the log-likelihood and the Bayesian Information Criterion (BIC).

Hierarchical Extension. The hierarchical extension of the Inverse Q-learning (HIQL) algorithm makes an important conceptual leap. It assumes that observed human trajectories are generated by a two-level process:

At the lower level, *intentions*—or latent reward functions r —determine the choice of actions a , which in turn govern the transition probabilities $P(s' | s, a)$ between states s . The transitions between intentions are modeled through a *discrete* Markov process with transition matrix Λ .



This is thus in contrast to previous approaches that assume *continuous* shifts in latent rewards. The active intention at any given time is unobserved. The model therefore does not output a fixed reward function to each individual but instead estimates *intention adoption probabilities*—the likelihood that a given behavior at time t was generated under each latent intention.

Notably, the shift from continuous to discrete transitions has improved model fit in recent studies of animal behavior. For our PGG data, this perspective may offer a potential explanation for the so-called “other” cluster, which often exhibits abrupt round-to-round changes in contribution patterns.

4 Data

We use data gathered from standard linear public good games across different game length horizons (7, 10, 20, and 30 rounds). All except the 20-round subsets contain

Table 3: First-Round Cooperation Types by Period Length.

Type Periods	7	10	20	30	Ours	T&V 2018
Free Rider (%)	14	16	23	9	14.0	19.2
Full Contributor (%)	12	39	26	43	27.6	10.4
Conditional Cooperator (%)	75	45	51	49	58.4	61.3

Note: Percentages based on first-round normalized contributions in our pooled dataset. Our dataset comprises 50,390 observations from 2,938 participants. Benchmark values from Thöni and Volk [40], based on 7,107 conditional-contribution observations (strategy method).

games without experimental intervention (like a punishment option, or a chat protocol). Furthermore, we only choose studies where the information treatment is such that players observe the *average contribution* of other team members after each round. Our dataset comprises 50,390 observations from 2,938 participants. Tab. S.2 provides details of the original studies and several focal parameters, such as group size, number of rounds, and participants per study. Fig. S.1 visualizes the raw data as a two-dimensional time series.

To assess the representativeness of our dataset, we classify participants based on their first-round contributions (Tab. 3). Following Cotla and Petrie [89], we use initial behavior as a proxy for social preference types². Using the thresholds from Thöni and Volk [40] — Free Riders ($c \leq 0.1$), Conditional Cooperators ($0.1 < c < 0.9$), and Full Cooperators ($c \geq 0.9$) — we find that Free Riders account for 14.0% (vs. 19.2% in the meta study), Conditional Cooperators for 58.4% (vs. 61.3%), and Full Cooperators for 27.6% (vs. 10.4%). While our dataset features more Full Cooperators and slightly fewer Conditional Cooperators, Conditional Cooperators remain the majority, indicating that our sample aligns well with canonical behavioral patterns.

5 Results

Within the full dataset, the 10-round games with four-person groups constitute the modal experimental design [90, 91]. Accordingly, Sections 5.1 and 5.2 are based on this 10-round subset only.

5.1 DTW-based Clustering Reveals Six Behavioral Clusters

We apply unsupervised learning to partition the multivariate time series data. The procedure consists of three steps: (1) selecting the *number of clusters*, (2) *computing distances* between time series, and (3) using these distances to *construct clusters*. For the 10-round subset, the optimal number of clusters is determined to be

²First-round contributions strongly correlate with unconditional strategy-method classifications [44, 89].

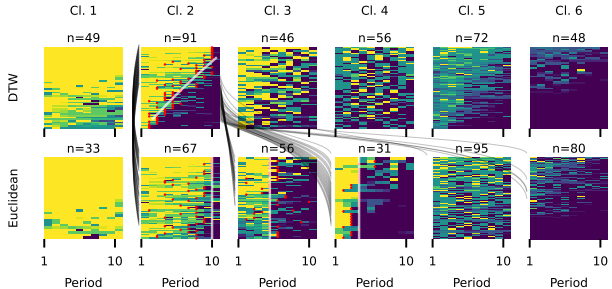


Figure 2: Global vs. Local Alignment. Participants are clustered based on two different distance metrics: DTW (global) and Euclidean (local) distance. Each small panel represents one cluster within a method, with participants sorted by their average contribution (highest on top). Red dots indicate when the most substantial consecutive drop in contribution occurs per participant. In the DTW cluster 2, a quadratic regression curve is overlaid to illustrate that the drop can occur at any point in the game. In the Euclidean clusters 2, 3, and 4, a vertical reference line is drawn to mark the period where most detected decline points are concentrated. Cell color encodes contribution magnitude (yellow indicates higher relative contribution, dark blue lower), and sample sizes per cluster appear above each panel.

six (see App. E.1). We adopt the same number of clusters when partitioning the remaining subsets (7, 20, and 30 rounds).

Global Alignment Outperforms Local Alignment. To illustrate the value of accommodating temporal misalignment when *computing distances*, we compare clustering results based on either local alignment (Euclidean distance) or global alignment (DTW; Fig. 2). DTW identifies a salient group (Cluster 2) characterized by a sharp transition from high to low contributions at different points in time. Under Euclidean distance, these participants are fragmented across multiple clusters based solely on when the switch occurs. In other words, Euclidean distance imposes artificial time-locking, whereas DTW correctly groups the shared strategic pattern of a qualitative shift from cooperation to defection (details in App. E.3).

Once DTW is selected as the appropriate similarity metric, varying the clustering algorithm results in only minor differences in the partition (App. E.4). We therefore adopt spectral clustering to *construct clusters*. The clustered raw data can be seen in the first row in Fig. 3. Finally, compared to established methods such as hierarchical clustering [39], C-Lasso [47], and finite mixture models [43], our approach produces the cleanest and most interpretable segmentation of behavioral types (Fig. S.6).

These analyses confirm that the identified clusters are not artifacts of specific modeling choices. We next assess whether they are also stable with respect to sampling

variation.

Clusters Are Robust to Sampling Variation Yet Retain Within-Cluster Heterogeneity. We assess cluster quality using bootstrap resampling (100 replications) and heterogeneity metrics. The clustering solution is highly stable: bootstrap partitions closely match the original assignment (ARI = 0.861, SD = 0.061; NMI = 0.868, SD = 0.047), and participants return to their dominant cluster in 29.9% of replications (SD = 3.3 pp), well above the 16.7% expected under random assignment (Tab. S.3).

At the same time, clusters intentionally retain substantial internal heterogeneity. Although all trajectories are assigned to one of six clusters, clusters explain only 29.5% of total DTW-based trajectory variance, leaving 70.5% within clusters. Individual fit varies widely: 26.9% of participants are closer to an alternative cluster than their assigned cluster (silhouette < 0), and between-cluster separation is modest (ratio = 1.56; see Tab. S.3).

Taken together, cluster assignments are robust to resampling yet leave ample room for the idiosyncratic and stochastic variation in individual contribution behavior that is well documented in the PGG literature.

5.2 Two Intentions Successfully Integrate Actions and States

To interpret the clusters, we estimate a latent variable model [82] based on the observed player contributions (actions) and the average contributions of their group members (states).

We find that increasing the number of latent intentions from one to two yields the largest improvement in test log-likelihood (LL), accompanied by the smallest increase in BIC (Δ LL = 0.66; Δ BIC = 75.2, Tab. S.5). We thus assume two latent intentions. Model fit on two latents across clusters is detailed in Tab. S.6, column 2.

Intentions Adoption Probabilities Allow for the Joint Interpretation of States and Actions. The latent-variable model outputs posterior intention adoption probabilities. Because this quantity is latent, it must be interpreted in relation to the observed player contributions (actions) and group average contributions (states). This relationship becomes clear when examining individual examples in Fig. S.10, where intention probabilities are plotted alongside actions and states. In some cases, intentions closely track behavioral choices; in others, they align more strongly with state dynamics. In other words, the intention adoption probabilities formally integrate both observable data—actions and states—into a single representational trajectory. This integration allows researchers to interpret participants' underlying decision tendencies without relying on ad

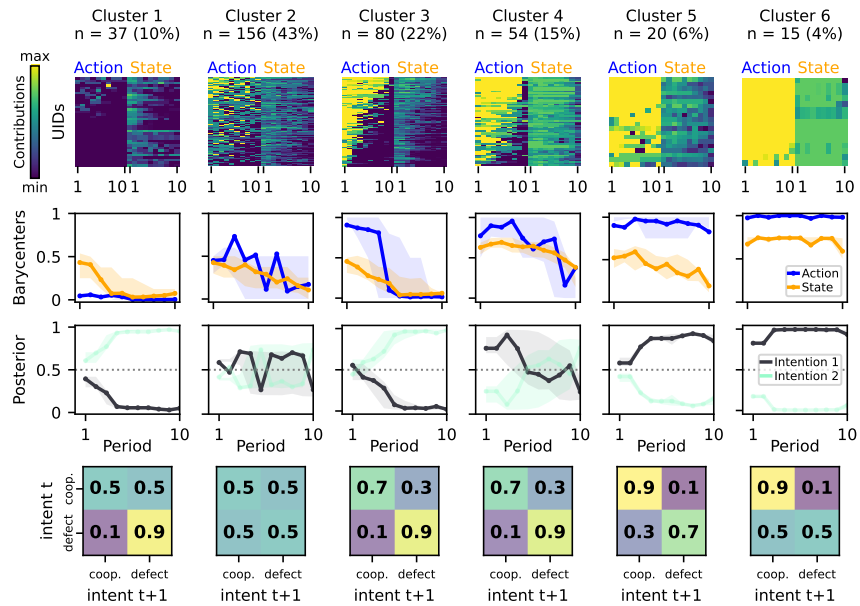


Figure 3: Clustering Analysis of Action-State Patterns and Intention Dynamics. (1) Heatmaps of action and state trajectories by cluster, ordered by mean action. Clustering uses two-dimensional time series of own contributions (action) and others’ average contributions (state), normalized to $[0,1]$. Rows denote individuals (UIDs), and rows as well as clusters are ordered from lowest to highest average contribution. (2) DTW barycenters of action-state patterns per cluster, with interquartile ranges shaded. (3) DTW barycenter averages of posterior intention adoption probabilities by cluster, with interquartile ranges shaded. Two intentions are estimated; the second is the complement of the first. Values closer to one indicate a higher likelihood that the intention is adopted. (5) Average transition probabilities between cooperative and defecting intentions per cluster.

hoc comparisons between separate state and action patterns.

Latent Intentions Successfully Model Stable and Switching Decision Patterns. We aggregate individual posterior trajectories within each cluster using Barycenter averaging (Fig. 3, row 3). Clusters 1, 5, and 6 display well-separated intention-adoption probabilities that change little after early rounds. This suggests that participants in these clusters form stable strategic intentions and adhere to them throughout the game.

In the behavioral data (Fig. 3, rows 1 and 2), these intentions correspond to persistent free-riding (Cluster 1) and sustained cooperation (Clusters 5–6). Cluster 1 exhibits uniformly low contributions, visible as a dark blue heatmap and a flat DTW barycenter near zero. In contrast, Cluster 6 shows consistently high contributions, with a near-uniform yellow heatmap and a barycenter that remains close to one throughout.

Because the model captures these established types, we can also interpret Cluster 2 with confidence. This group exhibits frequent alternation between cooperation and defection, often from one round to the next. Their inferred transition probabilities (Fig. 3, row 4) show a roughly 50% chance of switching intentions each period—indicating neither noise nor gradual learning, but a distinct decision-making mode characterized by

continuous strategy experimentation. We therefore refer to this behavioral type as “Switchers”: players who actively and frequently cycle between intentions.

The discrete latent-intention formulation thus provides a unified framework that accommodates both stable and erratic behavioral dynamics within the same generative process. It confirms long-known strategic types and additionally suggests that high-frequency intention switching constitutes a meaningful and interpretable behavioral pattern in its own right.

5.3 Interpretation of the Clusters

Overall, out of the six behavioral patterns, two maintain stable strategies. Cluster 1 represents persistent *free riders* who defect throughout despite favorable early outcomes, while Cluster 6 comprises *consistent cooperators* who sustain high contributions when experiencing positive feedback. Cluster 5 are *unconditional cooperators* who maintain high contributions even under unfavorable conditions. Note that the distinction between Clusters 5 and 6 becomes identifiable through DTW’s two-dimensional representation, which incorporates both an individual’s contributions and the surrounding group behavior. Our approach identifies these types across game lengths—free riders and consistent cooperators appear in all subsets, while uncondi-

tional cooperators emerge only in the shorter horizons. Please consult Fig. S.9 for a clear visual comparison of types/clusters across game lengths.

The remaining clusters reveal dynamic forms of cooperation breakdown. Cluster 3 consists of *threshold switchers* who begin with near-maximal cooperation but then abruptly transition to persistent free riding. This discontinuity is clearly visible in both the raw data (row 1) and barycenters (Fig. 3, row 2). The pattern resembles classical discontinuous adjustment mechanisms: *grim-trigger* strategies that cooperate until a perceived deviation and then punish permanently [92, 93], Win–Stay Lose–Shift rules that switch when outcomes fall below aspiration [94, 95], and adaptive-aspiration models generating endogenous switching thresholds [96]. However, unlike planned endgame defection, the switch in Cluster 3 does occur at any round, suggesting a reactive breakdown rather than horizon-based planning. This type is most clearly observed in the 10-round subset but also appears more weakly in the 30-round games.

Cluster 4 exhibits a noisier decline: players start with high cooperation but reduce contributions gradually, with full defection concentrated toward the final rounds. Patterns of high early cooperation followed by a sharp collapse near the end of the game are broadly consistent with the classic “endgame effect” in finitely repeated social dilemmas [e.g. 97–99]. In public-goods experiments, for instance, Gächter and Thöni [100] document groups that maintain substantial contributions up to the penultimate round and then free ride in the final period, and interpret this as rational last-round defection. Engel and Rockenbach [101] and Engel [102] interpret this behavior as *farsighted free-riders* who “feed the cow” by contributing in early periods and then “milk” it by cutting contributions once exploitation becomes profitable. Our Cluster 4 matches this pattern but is identified in a fully data-driven way.

Finally, *Cluster 2* appears erratic at first glance, but becomes interpretable under a latent-state perspective as *Switchers*. We examine this behavior in detail in the next subsection.

5.4 “Switchers” across subsets

To quantify the behavior of *Cluster 2* in Fig. 3, we define three properties of intention dynamics: *stickiness* (lag-1 autocorrelation), *switching rate* (intention transition probabilities), and *volatility* (posterior threshold crossings).

We define “Switchers” using three empirically-motivated thresholds: (1) *stickiness* < 0.15 (conventional threshold for weak temporal dependence), (2) *switching rate* > 0.35 (75th percentile, representing elevated but sub-random transition rates), and (3) *volatility* > 0.25 (indicating posterior reversals approximately

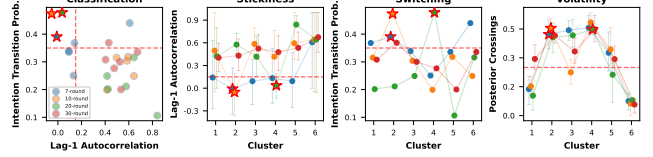


Figure 4: High-Switcher Identification Through Multi-Metric Behavioral Classification. (A) Classification of all 24 behavioral clusters across four game lengths (7, 10, 20, 30 rounds) in a two-dimensional space defined by *stickiness* (lag-1 autocorrelation) and *switching rate* (mean transition probability between latent cooperative and defective intentions). Switchers (stars) meet all three criteria. Dashed red lines show decision boundaries. (B–D) Cluster-level metrics with interquartile ranges (error bars). (B) Switchers exhibit near-zero stickiness. (C) Switching rates for Switchers (39–48%) approach random-walk behavior (50%), indicating frequent reversals in latent intention. (D) Posterior volatility reflects how often inferred intentions cross the 0.5 threshold. Only Switchers pair this with low stickiness and high switching.

every four rounds).

It is important to note that all three metrics need to be present to define the behavior of Cluster 2 because each metric alone fails to discriminate this behavior reliably.

Across datasets, *Switchers* emerge as a nontrivial share of participants. They appear in three of four game-length subsets: 456 participants in the 7-round subset (41%), 123 participants in the 10-round subset (34%), and 49 participants in the 20-round subset (10%). No clusters in the 30-round subset meet all three criteria. In total, Switchers represent 628 out of $N = 2938$ participants (21.4%). Their grouping via DTW-based trajectory similarity confirms they form a distinct cluster rather than residual outliers forced together.

Switchers show near-zero *stickiness*, *switching rate* rates close to 50%, and weak behavioral responsiveness to peers’ contributions ($r = 0.14$, compared with $r = 0.41$ in other types). The prevalence of *Switchers* declines systematically with game length: 41% in 7-round games, 34% in 10-round games, 10% in 20-round games, and 0% in 30-round games. This pattern may suggest early-stage strategic uncertainty that resolves as experience accumulates: In short interactions, many participants remain uncommitted and explore both strategic directions. When more time is available, they tend to converge toward stable cooperative or defective patterns.

6 Discussion

Our main contributions are twofold. First, we show that pattern-based alignment using Dynamic Time Warp-

ing (DTW) substantially improves behavioral clustering in repeated-game environments relative to conventional Euclidean alignment. By grouping trajectories according to their temporal shape rather than round-by-round proximity, we uncover structure in dynamic behavior that is both interpretable and theoretically meaningful. Second, we apply a latent-variable framework in which individuals switch *discretely* between intentions over time. By formally integrating the two observable time series, our approach provides a principled interpretation of each cluster. This approach recovers well-known behavioral types (such as persistent free riders and unconditional cooperators) that have been repeatedly validated in the literature, while also delivering the first rigorous account of the previously ambiguous “other” group.

A Unifying Framework. Our two-step approach provides a *unifying framework* for explaining *all* observed behavioral clusters in the PGG literature. Prior work typically imposes theory-driven assumptions that successfully capture a few well-established types, but then relegate the remaining behavior to error terms or “unexplained heterogeneity.” In contrast, every cluster we uncover is interpretable through the latent-variable structure: even the previously ambiguous “other” group receives a coherent interpretation via three key parameters—autocorrelation, transition probabilities, and intention crossings.

This unified perspective yields two particularly substantive insights for research on cooperation dynamics. First, we identify a clear class of *threshold switchers* who begin with near-maximal cooperation before abruptly transitioning to persistent free riding. Prior work has inferred such strategies either by restricting subjects to a pre-specified menu of strategies [e.g. 103], or by estimating behavior within narrow parametric classes such as memory-one HMMs [104] or finite-state automata [105]. By contrast, our identification operates directly on unconstrained contribution trajectories and recovers this cluster without any prior specification of memory length, state space, or strategy catalog. To our knowledge, this is the first purely data-driven recovery of a grim-trigger-like pattern from human play. Second, we show that a substantial fraction of individuals exhibit *volatile but recoverable* intention dynamics. It is important to interpret this behavior: Standard models treat defections as informative and persistent, triggering punishment and the collapse of cooperation. Our findings show that a substantial fraction of individuals exhibit volatile intention dynamics: deviations are frequent but reversible. In settings where cooperation underpins long-term value—supply chains, alliances, subscription services, customer retention, and online communities—misinterpreting such transient defections can destroy value by breaking *relationships that would have*

recovered. Recognizing intentional volatility expands the strategy space: forward-looking partners may rationally exercise *forgiveness and strategic patience*, maintaining cooperation because they expect switching types to return to cooperative behavior.

Managerial Relevance. Our framework is fully data-driven and therefore well-suited for settings where behavior is complex and controlled laboratory experimentation is infeasible. We benchmark its validity in a mature and robust literature and find that it reliably recovers well-established types and yields plausible interpretations for all patterns found. In this sense, the PGG environment functions as a stress test: if the method can reconstruct and interpret a space of behaviors that is already well understood, it becomes a credible tool for domains where theory remains underdeveloped. Behavioral finance provides a prime illustration. A wide variety of trading and portfolio archetypes has been documented—ranging from retail trader styles and high-frequency trading roles to mutual-fund strategies and depositor behavior in bank runs (see Tab. S.1). However, existing approaches often compress rich time-series behavior into engineered features or factor exposures, obscuring temporal structure and strategic heterogeneity. Our approach is designed to thrive in exactly such environments. Financial decisions generate large panel time-series datasets, and our method operates directly on the *full trajectories* rather than on prespecified summaries.

Straightforward Applicability. Our approach is designed for straightforward adoption. In practice, analysts only need to provide a panel of (potentially multidimensional) time series; the pipeline performs DTW-based clustering, followed by fitting the hierarchical inverse Q-learning. A central challenge is visualizing rich behavioral trajectories. Standard line plots become unreadable when many individuals are shown, and existing heatmaps often collapse the time dimension, often plotting state against actions. We therefore introduce an effective visualization scheme for multidimensional time series: raw trajectories are displayed as heatmaps sorted by average contribution. The sorting, in particular, makes behavioral patterns immediately visible even when they differ in timing or absolute levels. DTW-based barycenters are plotted alongside, preserving characteristic temporal structure without the over-smoothing inherent in simple averages. These elements make the workflow highly transferable. Practitioners can reuse our plotting tools, apply DTW-based spectral clustering to their own data, and interpret resulting clusters via the latent reward structure. All code will be made publicly available on GitHub.

Limitation. A natural limitation of our approach is that DTW clusters contribute sequences based on their observable temporal shape rather than on underlying intentions. This means that similar contribution paths may arise from different motives. In addition, DTW treats similar behaviors at different time points as comparable, an assumption that may be imperfect in finite-horizon games where the interpretation of actions can vary over time. We partially address this concern in the second stage by applying the HIQL model, which incorporates forward-looking behavior through Q-learning and discount factors that capture horizon effects. While this does not fully resolve the issue, it allows us to interpret DTW-based behavioral regularities through a model that explicitly accounts for temporal decision structure.

Future Work. Our model adapts reinforcement-learning tools developed for animal navigation to human cooperation. A natural extension is to integrate human-specific drivers—such as aspirations and affective responses—so that latent intentions more fully capture social motivations. Methodologically, we estimate inverse Q-learning *within* clusters; evaluating how results change without clustering, or with alternative segmentation, is an important next step. Allowing cluster-specific discount factors may also reveal differences in foresight, though lower values require additional smoothing to ensure convergence. Several technical refinements could improve estimation: incorporating first-round actions directly into state inference, aligning intention initialization with clear behavioral types (e.g., unconditional cooperators), and assessing alternative binning strategies to retain richer behavioral detail. Together, these extensions would increase psychological realism, robustness, and scalability to larger applied settings.

References

- [1] Christoph Engel. Tacit collusion: The neglected experimental evidence. *Journal of Empirical Legal Studies*, 12(3):537–577, 2015.
- [2] Terrence Hendershott, Charles M Jones, and Albert J Menkveld. Does algorithmic trading improve liquidity? *The Journal of finance*, 66(1):1–33, 2011.
- [3] Mathias Drehmann and Kleopatra Nikolaou. Funding liquidity risk: definition and measurement. *Journal of Banking & Finance*, 37(7):2173–2182, 2013. doi: 10.2139/ssrn.1338092.
- [4] Thomas B. King, Travis D. Nesmith, Anna Paulson, and Todd Prono. Central clearing and systemic liquidity risk. Finance and Economics Discussion Series 2020-009r1, Board of Governors of the Federal Reserve System, Washington, DC, 2022.
- [5] David M Kreps, Paul Milgrom, John Roberts, and Robert Wilson. Rational cooperation in the finitely repeated prisoners’ dilemma. *Journal of Economic Theory*, 27(2):245–252, 1982.
- [6] J. Ledyard. Public goods: A survey of experimental research. In J. Kagel and A. Roth, editors, *Handbook of Experimental Economics*, pages 253–279. Princeton University Press, 1995.
- [7] Jennifer Zelmer. Linear public goods experiments: A meta-analysis. *Experimental Economics*, 6(3):299–310, 2003. doi: 10.1023/a:1026277420119.
- [8] Ananish Chaudhuri. Sustaining cooperation in laboratory public goods experiments: a selective survey of the literature. *Experimental Economics*, 14(1):47–83, 2011. doi: 10.1007/s10683-010-9257-1.
- [9] Roberto Burlando and Francesco Guala. Heterogeneous agents in public goods experiments. *Experimental Economics*, 8(1):35–54, 2005. doi: 10.1007/s10683-005-0436-4.
- [10] C. F. Camerer and E. Fehr. When does “economic man” dominate social behavior? *Science*, 311(5757):47–52, 2006.
- [11] E. Fehr and S. Gächter. Altruistic punishment in humans. *Nature*, 415(6868):137–140, 2002. doi: 10.1038/415137a.
- [12] Urs Fischbacher and Simon Gächter. Social preferences, beliefs, and the dynamics of free riding in public good experiments. *American Economic Review*, 100(1):541–556, 2010. doi: 10.1257/aer.100.1.541.
- [13] A. Norenzayan and A. F. Shariff. The origin and evolution of religious prosociality. *Science*, 322(5898):58–62, 2008. doi: 10.1126/science.1158757.
- [14] James Andreoni. Cooperation in public goods experiments: Kindness or confusion. *American Economic Review*, 85(4):891–904, 1995.
- [15] D. Houser and R. Kurzban. Revisiting kindness and confusion in public goods experiments. *American Economic Review*, 92(4):1062–1069, 2002. doi: 10.1257/00028280260344605.
- [16] M. N. Burton-Chellew, C. El Mouden, and S. A. West. Conditional cooperation and confusion in public goods experiments. *Proceedings of the National Academy of Sciences*, 113(6):1291–1296, 2016.
- [17] M. N. Burton-Chellew and S. A. West. Prosocial preferences do not explain human cooperation in public goods games. *Proceedings of the National Academy of Sciences*, 110(6):216–221, 2013.
- [18] R. C. Bayer, E. Renner, and R. Sausgruber. Confusion and learning in the voluntary contributions game. *Experimental Economics*, 16(4):478–496, 2013. doi: 10.1007/s10683-012-9348-2.
- [19] P. J. Ferraro and C. A. Vossler. The source and significance of confusion in public goods experiments. *B.E. Journal of Economic Analysis and Policy*, 10(1):53, 2010. doi: 10.2202/1935-1682.2006.
- [20] Guangrong Wang, Jianbiao Li, Wenhua Wang, Xiaofei Niu, and Yue Wang. Confusion cannot explain cooperative behavior in public goods games. *Proceedings of the National Academy of Sciences*, 121(10):e2310109121, 2024.
- [21] Urs Fischbacher, Simon Gächter, and Ernst Fehr. Are people conditionally cooperative? evidence from a public goods experiment. *Economics Letters*, 71(3):397–404, 2001. doi: 10.1016/S0165-1765(01)00394-9.
- [22] Maxwell N Burton-Chellew, Victoire D’Amico, and Claire Guérin. The strategy method risks conflating confusion with a social preference for conditional cooperation in public goods games. *Games*, 13(6):69, 2022. doi: 10.3390/g13060069.
- [23] Johannes Abeler and Daniele Nosenzo. Self-selection into laboratory experiments: Pro-social motives versus monetary incentives. *Experimental Economics*, 18(2):195–214, 2015. doi: 10.1007/s10683-014-9397-9.
- [24] Jason A Aimone, Laurence R Iannaccone, Michael D Makowsky, and Jared Rubin. Endogenous group formation via unproductive costs. *The Review of Economic Studies*, 80(4):1215–1236, 2013. doi: 10.1093/restud/rdt017.
- [25] Robin Cubitt, Simon Gächter, and Simone Quercia. Conditional cooperation and betrayal aversion. *Journal of Economic Behavior & Organization*, 141:110–121, 2017. doi: 10.1016/j.jebo.2017.06.013.
- [26] Alexis Dariel and Nikos Nikiforakis. Cooperators and reciprocators: A within-subject analysis of pro-social behavior. *Economics Letters*, 122(2):163–166, 2014. doi: 10.1016/j.econlet.2013.10.033.
- [27] Urs Fischbacher, Simon Gächter, and Simone Quercia. The behavioral validity of the strategy method in public good experiments. *Journal of Economic Psychology*, 33(4):897–913, 2012. doi: 10.1016/j.jeop.2012.04.002.
- [28] Urs Fischbacher, Simon Schudy, and Sabrina Teyssier. Heterogeneous reactions to heterogeneity in returns from public goods. *Social Choice and Welfare*, 43(1):195–217, 2014. doi: 10.1007/s00355-013-0763-x.
- [29] Toke R Fosgaard, Lars G Hansen, and Erik Wengström. Understanding the nature of cooperation variability. *Journal of Public Economics*, 120:134–143, 2014. doi: 10.1016/j.jpubeco.2014.09.004.
- [30] Simon Gächter, Felix Kölle, and Simone Quercia. Reciprocity and the tragedies of maintaining and providing the commons. *Nature Human Behaviour*, 1(9):650–656, 2017. doi: 10.1038/s41562-017-0191-5.
- [31] Benedikt Herrmann and Christian Thöni. Measuring conditional cooperation: A replication study in russia.

Experimental Economics, 12(1):87–92, 2009. doi: 10.1007/s10683-008-9197-1.

[32] Kenju Kamei. From locality to continent: A comment on the generalization of an experimental study. *Journal of Socio-Economics*, 41(2):207–210, 2012. doi: 10.1016/j.socec.2011.12.005.

[33] Martin G Kocher, Todd L Cherry, Stephan Kroll, Robert J Netzer, and Matthias Sutter. Conditional cooperation on three continents. *Economics Letters*, 101(3):175–178, 2008. doi: 10.1016/j.econlet.2008.07.015.

[34] Michael D Makowsky, William H Orman, and Sandra J Peart. Playing with other people’s money: Contributions to public goods by trustees. *Journal of Behavioral and Experimental Economics*, 53:44–55, 2014. doi: 10.1016/j.socec.2014.08.003.

[35] Christian Thöni, Jean-Robert Tyran, and Erik Wengström. Microfoundations of social capital. *Journal of Public Economics*, 96(7–8):635–643, 2012. doi: 10.1016/j.jpubeco.2012.04.003.

[36] Niels van Miltenburg, Vincent Buskens, Davide Barrera, and Werner Raub. Implementing punishment and reward in the public goods game: The effect of individual and collective decision rules. *International Journal of the Commons*, 8(1):47–78, 2014. doi: 10.18352/ijc.397.

[37] Stephan Volk, Christian Thöni, and Winfried Ruigrok. Temporal stability and psychological foundations of cooperation preferences. *Journal of Economic Behavior & Organization*, 81(2):664–676, 2012. doi: 10.1016/j.jebo.2011.10.006.

[38] Timo O Weber, Ori Weisel, and Simon Gächter. Dispositional free riders do not free ride on punishment. *Nature Communications*, 9(1):2390, 2018. doi: 10.1038/s41467-018-04775-8.

[39] Francesco Fallucchi, Richard A Luccasen, and Theodore L Turocy. Identifying discrete behavioural types: a re-analysis of public goods game contributions by hierarchical clustering. *Journal of the Economic Science Association*, 5(2):238–254, 2019. doi: 10.1007/s40881-018-0060-7.

[40] Christian Thöni and Stefan Volk. Conditional cooperation: Review and refinement. *Economics Letters*, 171:37–40, 2018. doi: 10.1016/j.econlet.2018.06.022.

[41] Robert Kurzban and Daniel Houser. Individual differences in cooperation in a circular public goods game. *European Journal of Personality*, 15(S1):S37–S52, 2001. doi: 10.1002/per.420.

[42] Robert Kurzban and Daniel Houser. Experiments investigating cooperative types in humans: A complement to evolutionary theory and simulations. *Proceedings of the National Academy of Sciences*, 102(5):1803–1807, 2005. doi: 10.1073/pnas.0408759102.

[43] Nicholas Bardsley and Peter G Moffatt. The metrics of public goods: Inferring motivations from contributions. *Theory and Decision*, 62(2):161–193, 2007. doi: 10.1007/s11238-006-9013-3.

[44] Laurent Muller, Martin Sefton, Richard Steinberg, and Lise Vesterlund. Strategic behavior and learning in repeated voluntary contribution experiments. *Journal of Economic Behavior & Organization*, 67(3):782–793, 2008.

[45] Daniel Houser, Michael Keane, and Kevin McCabe. Behavior in a dynamic decision problem: an analysis of experimental evidence using a bayesian type classification algorithm. *Econometrica*, 72(3):781–822, 2004. doi: 10.1111/j.1468-0262.2004.00512.x.

[46] Friedel Bolle and Jonathan HW Tan. Behavioral types of the dark side: identifying heterogeneous conflict strategies. *Journal of the Economic Science Association*, 7(1):49–63, 2021. doi: 10.1007/s40881-021-00101-z.

[47] Liangjun Su, Zhentao Shi, and Peter CB Phillips. Identifying latent structures in panel data. *Econometrica*, 84(6):2215–2264, 2016. doi: 10.2139/ssrn.2448189.

[48] Sebastian Bordt and Helmut Farbmacher. Estimating grouped patterns of heterogeneity in repeated public goods experiments. Working Paper, 2019.

[49] Christoph Engel. Estimating heterogeneous reactions to experimental treatments. Working paper, 2020.

[50] Francesco Fallucchi, Andrea Mercatanti, and Jan Niederreiter. Identifying types in contest experiments. *International Journal of Game Theory*, 50(1):39–61, 2021. doi: 10.1007/s00182-020-00738-w.

[51] Brad M. Barber and Terrance Odean. Boys will be boys: Gender, overconfidence, and common stock investment. *Quarterly Journal of Economics*, 116(1):261–292, 2001. doi: 10.2139/ssrn.139415.

[52] Alok Kumar. Who gambles in the stock market? *Journal of Finance*, 64(4):1889–1933, 2009. doi: 10.1111/j.1540-6261.2009.01483.x.

[53] Daniel Dorn and Paul Sengmueller. Trading as entertainment? *Management Science*, 55(4):591–603, 2009.

[54] Andrei A. Kirilenko, Albert S. Kyle, Mehrdad Samadi, and Tugkan Tuzun. The flash crash: The impact of high-frequency trading on an electronic market. *Journal of Finance*, 72(3):967–998, 2017.

[55] Jonathan Brogaard, Terrence Hendershott, and Ryan Riordan. High-frequency trading and its impact on market quality. *Review of Financial Studies*, 27(8):2267–2306, 2014.

[56] Laurent E Calvet, John Y Campbell, and Paolo Sodini. Measuring the financial sophistication of households. *American Economic Review*, 99(2):393–398, 2009. doi: 10.3386/w14699.

[57] Keith C. Brown, W. Van Harlow, and Laura T. Starks. Of tournaments and temptations: An analysis of managerial incentives in the mutual fund industry. *Journal of Finance*, 51(1):85–110, 1996. doi: 10.2307/2329303.

[58] Russ Wermers. Mutual fund performance: An empirical decomposition into stock-picking talent, style, transactions costs, and expenses. *Journal of Finance*, 55(4):1655–1695, 2000. doi: 10.2469/dig.v31.n1.836.

[59] Rajkamal Iyer and Manju Puri. Understanding bank runs: The importance of depositor-bank relationships and networks. *American Economic Review*, 102(4):1414–1445, 2012.

[60] Stefan T. Trautmann and Razvan Vlahu. Bank-run psychology. *Review of Finance*, 17(2):971–1000, 2011.

[61] Gary Gorton. *Misunderstanding Financial Crises: Why We Don’t See Them Coming*. Oxford University Press, 2012.

[62] Ido Erev and Alvin E Roth. Predicting how people play games: Reinforcement learning in experimental games with unique, mixed strategy equilibria. *American Economic Review*, 88(4):848–881, 1998.

[63] Colin Camerer and Teck-Hua Ho. Experience-weighted attraction learning in normal form games. *Econometrica*, 67(4):827–874, 1999. doi: 10.1111/1468-0262.00054.

[64] Teck-Hua Ho, Colin Camerer, and Juin-Kuan Chong. Self-tuning experience-weighted attraction learning in games. *Econometrica*, 75(5):1375–1416, 2007.

[65] Antonio Rangel, Colin Camerer, and P. Read Montague. A framework for studying the neurobiology of value-based decision making. *Nature Reviews Neuroscience*, 9(7):545–556, 2008. doi: 10.1038/nrn2357.

[66] Arthur Dolgopolov. Reinforcement learning in a prisoner’s dilemma. *Games and Economic Behavior*, 144: 84–103, 2024.

[67] Guozhong Zheng, Jiqiang Zhang, Shengfeng Deng, Weiran Cai, and Li Chen. Evolution of cooperation in the public goods game with q-learning. *Chaos, Solitons and Fractals*, 188:115568, 2024. doi: 10.1016/j.chaos.2023.115568.

[68] Ernst Fehr and Klaus M Schmidt. A theory of fairness, competition, and cooperation. *The quarterly journal of economics*, 114(3):817–868, 1999.

[69] Matthew Rabin. Incorporating fairness into game theory and economics. *The American economic review*, pages 1281–1302, 1993. doi: 10.2307/j.ctvcm4j8j.15.

[70] Mansour Alyahay, Gabriel Kalweit, Maria Kalweit, Golan Karvat, Julian Ammer, Artur Schneider, Ahmed Adzemovic, Andreas Vlachos, Joschka Boedecker, and Ilka Diester. Mechanisms of premotor-motor cortex interactions during goal directed behavior. *bioRxiv*, pages 2023–01, 2023. doi: 10.1101/2023.01.20.524944. Preprint.

[71] Matthew Rosenberg, Tony Zhang, Pietro Perona, and Markus Meister. Mice in a labyrinth show rapid learning, sudden insight, and efficient exploration. *eLife*, 10:e66175, 2021. doi: 10.7554/eLife.66175.

[72] Andrew Y. Ng and Stuart J. Russell. Algorithms for inverse reinforcement learning. In *International Conference on Machine Learning (ICML)*, volume 1, page 2, 2000.

[73] Saurabh Arora and Prashant Doshi. A survey of inverse reinforcement learning: Challenges, methods and progress. *Artificial Intelligence*, 297:103500, 2021. doi: 10.1016/j.artint.2021.103500.

[74] Sateesh Kumar, Jonathan Zamora, Nicklas Hansen, Rishabh Jangir, and Xiaolong Wang. Graph inverse reinforcement learning from diverse videos. In *Conference on Robot Learning*, pages 55–66. PMLR, 2023.

[75] Jiayu Chen, Tian Lan, and Vaneet Aggarwal. Option-aware adversarial inverse reinforcement learning for robotic control. In *2023 IEEE International Conference on Robotics and Automation (ICRA)*, pages 5902–5908. IEEE, 2023. doi: 10.1109/icra48891.2023.10160374.

[76] Gabriel Kalweit, Maria Huegle, Moritz Werling, and Joschka Boedecker. Deep inverse q-learning with constraints. *Advances in Neural Information Processing Systems*, 33:14291–14302, 2020.

[77] Payam Nasernejad, Tarek Sayed, and Rushdi Al-saleh. Multiagent modeling of pedestrian-vehicle conflicts using adversarial inverse reinforcement learning. *Transportmetrica A: Transport Science*, 19(3): 2061081, 2023. doi: 10.1080/23249935.2022.2061081.

[78] Shoichiro Yamaguchi, Honda Naoki, Muneki Ikeda, Yuki Tsukada, Shunji Nakano, Ikue Mori, and Shin Ishii. Identification of animal behavioral strategies by inverse reinforcement learning. *PLoS Computational Biology*, 14(5):e1006122, 2018. doi: 10.1101/129007.

[79] Minhae Kwon, Saurabh Daptardar, Paul R. Schrater, and Xaq Pitkow. Inverse rational control with partially observable continuous nonlinear dynamics. In *Advances in Neural Information Processing Systems*, volume 33, pages 7898–7909, 2020.

[80] Zoe Ashwood, Aditi Jha, and Jonathan W Pillow. Dynamic inverse reinforcement learning for characterizing animal behavior. *Advances in Neural Information Processing Systems*, 35:29663–29676, 2022.

[81] Zoe C. Ashwood, Nicholas A. Roy, Iris R. Stone, International Brain Laboratory, Anne E. Urai, Anne K. Churchland, Alexandre Pouget, and Jonathan W. Pillow. Mice alternate between discrete strategies during perceptual decision-making. *Nature Neuroscience*, 25(2):201–212, 2022. doi: 10.1101/2020.10.19.346353.

[82] Hao Zhu, Brice De La Crompe, Gabriel Kalweit, Artur Schneider, Maria Kalweit, Ilka Diester, and Joschka Boedecker. Multi-intention inverse q-learning for interpretable behavior representation. *Transactions on Machine Learning Research*, 2024. Available online: <https://openreview.net/forum?id=hrKHkmLUFk>.

[83] Colin Camerer, Teck Ho, and Kuan Chong. Models of thinking, learning, and teaching in games. *American Economic Review*, 93(2):192–195, 2003. doi: 10.1257/000282803321947038.

[84] Sendhil Mullainathan and Jann Spiess. Machine learning: an applied econometric approach. *Journal of Economic Perspectives*, 31(2):87–106, 2017. doi: 10.1257/jep.31.2.87.

[85] Donald J. Berndt and James Clifford. Using dynamic time warping to find patterns in time series. In *Proceedings of the 3rd International Conference on Knowledge Discovery and Data Mining (KDD Workshop)*, pages 359–370, Seattle, WA, USA, 1994.

[86] Ulrike Von Luxburg, Robert C Williamson, and Isabelle Guyon. Clustering: Science or art? In *Proceedings of ICML workshop on unsupervised and transfer learning*, pages 65–79. JMLR Workshop and Conference Proceedings, 2012.

[87] Olatz Arbelaitz, Ibai Gurrutxaga, Javier Muguerza, Jesús M Pérez, and Iñigo Perona. An extensive comparative study of cluster validity indices. *Pattern Recognition*, 46(1):243–256, 2013. doi: 10.1016/j.patcog.2012.07.021.

[88] François Petitjean, Alain Ketterlin, and Pierre Gançarski. A global averaging method for dynamic time warping, with applications to clustering. *Pattern recognition*, 44(3):678–693, 2011. doi: 10.1016/j.patcog.2010.09.013.

[89] Chenna Reddy Cotla and Ragan Petrie. Social preferences and payoff-based learning explain contributions in repeated public goods games. Working paper, 2019. URL http://www.raganpetrie.org/uploads/8/4/4/3/84436206/prefs_and_learning_paper_nov2019.pdf.

[90] John O. Ledyard. Public goods: A survey of experimental research. In John H. Kagel and Alvin E. Roth, editors, *Handbook of Experimental Economics*, pages 111–194. Princeton University Press, 1995.

[91] Ananish Chaudhuri. Sustaining cooperation in laboratory public goods experiments: a selective survey of the literature. *Experimental Economics*, 14(1):47–83, 2011. doi: 10.1007/s10683-010-9257-1.

[92] James W. Friedman. A non-cooperative equilibrium for supergames. *The Review of Economic Studies*, 38(1):1–12, 1971. doi: 10.1017/cbo9780511528231.011.

[93] Robert Axelrod. *The Evolution of Cooperation*. Basic Books, 1984.

[94] Martin Nowak and Karl Sigmund. A strategy of win-stay, lose-shift that outperforms tit-for-tat in the prisoner’s dilemma. *Nature*, 364(6432):56–58, 1993.

[95] Michael W. Macy and Andreas Flache. Learning dynamics in social dilemmas. *Proceedings of the National Academy of Sciences*, 99(Suppl 3):7229–7236, 2002. doi: 10.1007/springerreference_301922.

[96] Rajiv Karandikar, Dilip Mookherjee, Debraj Ray, and Fernando Vega-Redondo. Evolving aspirations and cooperation. *Journal of Economic Theory*, 80(2):292–331, 1998. doi: 10.1006/jeth.1997.2379.

[97] Claudia Keser and Frans van Winden. Conditional cooperation and voluntary contributions to public goods. *Scandinavian Journal of Economics*, 102(1):23–39, 2000.

[98] Simon Gächter. Conditional cooperation: Behavioral regularities from the lab and the field and their policy implications. In *Economics and Psychology: A Promising New Cross-Disciplinary Field*, pages 19–50, 2007. doi: 10.7551/mitpress/2604.003.0006.

[99] Matthew Embrey, Guillaume R Fréchette, and Seda Yuksel. Cooperation in the finitely repeated prisoner’s dilemma. *American Economic Review*, 107(12):3267–3295, 2017.

[100] Simon Gächter and Christian Thöni. Social learning and voluntary cooperation among like-minded people. *Journal of the European Economic Association*, 3(2-3):303–314, 2005. doi: 10.2139/ssrn.632964.

[101] Christoph Engel and Bettina Rockenbach. Building and milking the public good: Farsightedness in voluntary contribution experiments. *Preprint*, 2020. Max Planck Institute Discussion Paper.

[102] Christoph Engel. What makes cooperation precarious? *Frontiers in Behavioral Economics*, 101:102712, 2024. doi: 10.1016/j.jeop.2024.102712. Forthcoming.

[103] Pedro Dal Bó and Guillaume R Fréchette. Strategy choice in the infinitely repeated prisoner’s dilemma. *American Economic Review*, 109(11):3929–3952, 2019. doi: 10.1257/aer.20181480.

[104] Eladio Montero-Porras, Jelena Grujić, Elias Fernández Domingos, and Tom Lenaerts. Inferring strategies from observations in long iterated prisoner’s dilemma experiments. *Scientific reports*, 12(1):7589, 2022. doi: 10.1038/s41598-022-11654-2.

[105] Max Kleiman-Weiner, Joshua B. Tenenbaum, and Pang Zhou. Non-parametric bayesian inference of strategies in repeated games. *Econometrics Journal*, 21(3):298–315, 2018. doi: 10.1111/ectj.12112.

[106] Antoni Bosch-Domenech, Jose G Montalvo, Rosemarie Nagel, and Albert Satorra. A finite mixture analysis of beauty-contest data using generalized beta distributions. *Experimental Economics*, 13(4):461–475, 2010. doi: 10.1007/s10683-010-9251-7.

[107] Anna Conte, John D Hey, and Peter G Moffatt. Mixture models of choice under risk. *Journal of Econometrics*, 162(1):79–88, 2011. doi: 10.1142/9789813235816-0001.

[108] Isabelle Brocas, Juan D Carrillo, Stephanie W Wang, and Colin F Camerer. Imperfect choice or imperfect attention? understanding strategic thinking in private information games. *Review of Economic Studies*, 81(3):944–970, 2014. doi: 10.1093/restud/rdu001.

[109] Mohamed A El-Gamal and David M Grether. Are people bayesian? uncovering behavioral strategies. *Journal of the American Statistical Association*, 90(432):1137–1145, 1995. doi: 10.2307/2291506.

[110] Pauli Virtanen, Ralf Gommers, Travis E. Oliphant, Matt Haberland, Tyler Reddy, David Cournapeau, Evgeni Burovski, Pearu Peterson, Warren Weckesser, Jonathan Bright, Stéfan J. van der Walt, Matthew Brett, Joshua Wilson, K. Jarrod Millman, Nikolay Mayorov, Andrew R. J. Nelson, Eric Jones, Robert Kern, Eric Larson, Christopher J. Carey, Ilhan Polat, Yu Feng, Eric W. Moore, Jake VanderPlas, Denis Laxalde, Josef Perktold, Robert Cimrman, Ian Henriksen, E. A. Quintero, Charles R. Harris, Anne M. Archibald, Antônio H. Ribeiro, Fabian Pedregosa, Paul van Mulbregt, and SciPy 1.0 Contributors. SciPy 1.0: Fundamental algorithms for scientific computing in python. *Nature Methods*, 17(3):261–272, 2020. doi: 10.1038/s41592-019-0686-2.

[111] Johannes Diederich, Timo Goeschl, and Israel Waichman. Group size and the (in)efficiency of pure public good provision. *European Economic Review*, 85:272–287, 2016. doi: 10.1016/j.eurocorev.2016.03.001.

[112] Christoph Engel, Sebastian Kube, and Michael Kurschilgen. Managing expectations: How selective information affects cooperation and punishment in social dilemma games. *Journal of Economic Behavior & Organization*, 187:111–136, 2021. doi: 10.1016/j.jebo.2021.04.029.

[113] Christoph Engel and Bettina Rockenbach. Give everybody a voice! the power of voting in a public goods experiment with externalities. MPI Collective Goods Preprint 2014/16, Max Planck Institute for Research on Collective Goods, November 2014. URL <https://ssrn.com/abstract=2519479>.

[114] Nikos Nikiforakis and Hans-Theo Normann. A comparative statics analysis of punishment in public-good experiments. *Experimental Economics*, 11(4):358–369, 2008. doi: 10.2139/ssrn.747144.

[115] Christoph Engel and Bettina Rockenbach. What makes cooperation precarious? *Journal of Economic*

Psychology, 101:102712, 2024. doi: 10.1016/j.joep.2024.102712.

[116] Michael Kosfeld, Akira Okada, and Arno Riedl. Institution formation in public goods games. *American Economic Review*, 99(4):1335–55, 2009. doi: 10.26481/umamet.2006029.

[117] Christoph Engel, Martin Beckenkamp, Andreas Glöckner, Bernd Irlenbusch, Heike Hennig-Schmidt, Sebastian Kube, Michael Kurschilgen, Alexander Morell, Andreas Nicklisch, Hans-Theo Normann, et al. First impressions are more important than early intervention: qualifying broken windows theory in the lab. *International Review of Law and Economics*, 37:126–136, 2014. doi: 10.1016/j.irle.2013.07.005.

[118] Christoph Engel and Michael Kurschilgen. The co-evolution of behavior and normative expectations: An experiment. *American law and economics review*, 15(2):578–609, 2013. doi: 10.1093/aler/aht010.

[119] Christoph Engel and Michael Kurschilgen. Aim high or aim low: The power of self-set normative goals in a social dilemma. Draft version, January 2019, 2019.

[120] Christoph Engel and Michael Kurschilgen. The fragility of a nudge: the power of self-set norms to contain a social dilemma. *Journal of Economic Psychology*, 81:102293, 2020. doi: 10.1016/j.joep.2020.102293.

[121] Peter J. Rousseeuw. Silhouettes: a graphical aid to the interpretation and validation of cluster analysis. *Journal of Computational and Applied Mathematics*, 20:53–65, 1987. doi: 10.1016/0377-0427(87)90125-7.

[122] Tadeusz Caliński and Jerzy Harabasz. A dendrite method for cluster analysis. *Communications in Statistics-theory and Methods*, 3(1):1–27, 1974. doi: 10.1080/03610917408548446.

[123] Anil K. Jain, M. Narasimha Murty, and Patrick J. Flynn. Data clustering: A review. *ACM Computing Surveys (CSUR)*, 31(3):264–323, 1999.

[124] Christian Hennig. What are the true clusters? *Pattern Recognition Letters*, 64:53–62, 2015. doi: 10.1016/j.patrec.2015.04.009.

[125] R. Mark Isaac and James M. Walker. Group size effects in public goods provision: The voluntary contributions mechanism. *The Quarterly Journal of Economics*, 103(1):179–199, 1988.

[126] Hao Zhu, Jasper Hoffmann, Baohe Zhang, and Joschka Boedecker. Fitting reinforcement learning model to behavioral data under bandits. *arXiv preprint arXiv:2511.04454v1*, pages 353–376, 2025.

Supplementary Materials

A Details on Methods

Several approaches have been proposed to classify behavioral types in PGGs. These approaches differ primarily along two dimensions: their reliance on theoretical assumptions (vs. purely data-driven approaches), and how they accommodate the inherent temporal structure of behavioral data.

At the theory-driven end, *finite mixture models* are widely used: Applications include PGGs [43], beauty contest experiments [106], lottery-choice tasks [107], and private-information games [108].

Similarly, *Bayesian mixture models* have gained traction for identifying latent behavioral types, particularly in PGGs [45] and probabilistic updating tasks [109]. These methods typically follow a three-stage procedure: first, specifying a parametric model of individual decision-making; second, estimating individual-specific parameters via Bayesian inference; and third, clustering these parameters post-estimation to delineate distinct behavioral types.

C-Lasso [47] extends this logic by merging estimation and clustering into a unified penalized regression framework. Instead of sequentially estimating parameters and clustering afterward, C-Lasso shrinks parameter estimates toward common values and thus implicitly groups subjects during estimation. This method has notably identified heterogeneous behaviors in contest experiments [50].

At the opposite, data-driven end of the spectrum lie unsupervised machine learning methods, such as *clustering algorithms* employed by Fallucchi et al. [39], Bolle and Tan [46] in analyzing social dilemmas. From an econometric perspective, these clustering methods function as dimensionality-reduction tools, uncovering latent behavioral patterns without predefined assumptions on distributions or preferences.

Instead of comparing points strictly by index, *DTW* aligns key structural moments—such as peaks—by warping the time dimension to minimize the overall alignment cost [see 85, for details]. Formally, for two time series, $\mathbf{x} = \{x_1, x_2, \dots, x_T\}$ and $\mathbf{y} = \{y_1, y_2, \dots, y_T\}$, DTW constructs a cost matrix D where each element $D(i, j)$ represents the cumulative cost of aligning x_i with y_j . The recurrence relation for computing $D(i, j)$ is given by

$$\begin{aligned} D(i, j) = & d(x_i, y_j) \\ & + \min \{D(i - 1, j), D(i, j - 1), D(i - 1, j - 1)\}, \end{aligned}$$

where the local distance $d(x_i, y_j)$ is typically defined as the squared difference $(x_i - y_j)^2$. The optimal DTW distance is then given by $D(T, T)$, found at the bottom-right corner of the matrix, which represents the minimal cumulative alignment cost.

B Types in Behavioral Finance

Table S.1: Use of Time-Series Data and Type Identification Methods in Behavioral Finance.

Paper	Time Series Used	How Time Series Are Processed	Type Method	Identification	Types Identified
Barber and Odean [51]	Trading history	Aggregated into turnover, returns, performance measures	Behavioral signature inference (no clustering)		Overconfident vs. less overconfident
Barber and Odean [51]	Trading history	Aggregated into turnover, returns, performance measures	Behavioral signature inference (no clustering)		Overconfident vs. less overconfident
Kumar [52]	Trade sequences	Collapsed into lottery-preference index	Preference-based econometric scoring		Lottery-seeking vs. non-gamblers
Dorn and Sengmueller [53]	Trading frequency	Reduced to counts and averages	Descriptive segmentation		Entertainment traders vs. others
Calvet et al. [56]	Portfolio histories	Used in the structural model of portfolio choice	Structural posterior classification		Sophisticated vs. unsophisticated investors
Kirilenko et al. [54]	HFT order flow	Engineered features (inventory, cancellations, message rates)	Unsupervised clustering (k-means)		Market makers, opportunistic traders, directional traders
Brogaard et al. [55]	HFT quotes & inventory	Aggregated into liquidity-supply ratios	Rule-based classification		Liquidity providers vs. liquidity takers
Brown et al. [57]	Fund returns	Estimated changing factor loadings and risk exposure over time	Structural/Regression-based style analysis		Risk-shifters, conservative, tournament-driven managers
Wermers [58]	Fund returns & holdings	Performance decomposition over time	Component-based classification		Stock pickers vs. style-driven funds
Iyer and Puri [59]	Withdrawal timing	Hazard/survival modeling of sequences	Regression-based segmentation		Early, conditional, late withdrawers
Trautmann and Vlahu [60]	Experimental round decisions	Strategy-method elicitation & decision sequences	Rule-based or simple mixture modeling		Run-prone, cautious, strategic waiters
Gorton [61]	Crisis dynamics	Descriptive analysis of crisis time series	Conceptual typology		Run-prone, strategic waiters, fundamentalists

Note: This literature typically reduces behavioral trajectories to engineered features, summary statistics, or factor loadings, instead of using the complete time series.

C Implementation Details of the HIQL Model

Fitting Process: We discretize the continuous range $[0, 1]$ of own contributions and others' contributions into five bins, which we denote as the action set $\mathcal{A} = \{a_1, a_2, a_3, a_4, a_5\}$ (five bins in $[0, 1]$). Similarly, we denote the state set as $\mathcal{S} = \{s_1, s_2, s_3, s_4, s_5\}$ (five bins in $[0, 1]$). The binning has the primary purpose of reducing the size of the Q-table. The original action set has, on average, 11 bins (in the canonical public good game, participants have an endowment of 10 tokens, and may contribute between 0 and 10 tokens to the joint project). As states are averages, their space is even larger. As defined earlier, the input for the model is time series trajectories (per participant) of state-action-next state triplets.

Following Zhu et al. [82], we employ a multi-stage fitting procedure. For all steps, we set the discount factor to $\gamma = 0.99$.

In the first stage, we run multiple HIQL fits with different numbers of intentions $K = 2, \dots, 5$ on the non-clustered dataset to obtain a global fit. We split this data into a train/test set. Reward functions are estimated on the training set, and predictive performance is evaluated on the test set using the out-of-sample/test log-likelihood. The choice of K is based on this predictive performance and the Bayesian Information Criterion (BIC). For each fitting, we perform 10 different initializations and select the best-performing initialization. The initial intention distribution Π is initialized uniformly, and the intention transition matrix Λ is initialized according to Zhu et al. [82] as $\Lambda = 0.95 \times I + N(0, 0.05 \times I)$ where N denotes the normal distribution and $I \in \mathbb{R}^{K \times K}$ is the identity matrix. This initial Λ is then normalized so that each row adds up to 1.

In the second stage of the fitting procedure, we obtain an independent but aligned HIQL fit for each cluster. Specifically, we initialize each cluster's HIQL model using the best global parameters (the global prior over initial latent intentions and the global transition probabilities between intentions across time) learned from all data combined. Using these as initialization ensures that all cluster-specific models start from a consistent baseline of how intentions are expected to emerge and evolve, while allowing each cluster to adapt its own intention-specific policies and rewards to reflect the behavioral characteristics of participants within that cluster.

As in Zhu et al. [82], we apply a five-fold cross-validation approach, and additionally implement a repeated stratified fold split. The stratification is based on the average contribution of individuals. We bin the clusters into three average contribution bins and ensure that both the training and test sets are sampled from all bins. Furthermore, we repeat this process ten times within each fold to obtain stable posterior estimates per participant.

Assessing Model Fit: Model fit is evaluated using the log-likelihood (LL), which quantifies how well the learned model explains the observed actions given the states. Because IRL models behavior probabilistically—estimating the likelihood that a participant selects a given action under a latent policy—the LL serves as a natural and sufficient measure of model performance. Higher (less negative) log-likelihood values indicate that the model assigns greater probability to the actions actually observed, meaning it captures participants' decision patterns more accurately. Conversely, lower log-likelihood values reflect greater behavioral noise or variability, as the model must distribute probability more diffusely across possible actions.

Aligning Latents: The main challenge in any latent-variable model lies in interpreting and aligning the latent dimensions. Because we estimate separate HIQL models for each behavioral cluster, the latent intentions are not automatically aligned across clusters—or across different folds and repetitions in cross-validation. To establish consistent labeling of intentions, we first visualize each participant's input data (states and actions) together with their inferred latent intentions. From these visualizations, we interpret the two dominant latent dimensions as reflecting *cooperative* and *defective* intentions. Accordingly, peaks and valleys in the action time series correspond to rises and falls in the inferred cooperation intention. Next, we apply a peak-detection algorithm [110] to identify peaks in both the action and latent-intention time series. Within each cluster, we then quantify how often each posterior intention aligns with the detected behavioral peaks. The intention showing the highest alignment is designated as *intention 1*.

D Details on the Data

Table S.2: Data Overview by Period Length.

Period Length	Study	Group Size	Participants
7	Diederich et al. [111]	10	410
	Diederich et al. [111]	40	200
	Diederich et al. [111]	100	500
	<i>Subset Total</i>	1110	
10	Engel et al. [112]	4	236
	Engel and Rockenbach [113]	4	102
	Nikiforakis and Normann [114]	4	24
	Diederich et al. [111]	40	200
	<i>Subset Total</i>	562	
20	Engel and Rockenbach [115]	3	30
	Engel and Rockenbach [115]	5	252
	Kosfeld et al. [116]	4	216
	<i>Subset Total</i>	498	
30	Engel et al. [117]	4	228
	Engel and Kurschilgen [118]	4	20
	Engel and Kurschilgen [119]	4	288
	Engel and Kurschilgen [120]	4	432
	<i>Subset Total</i>	968	
Grand Total		2938	

Note: Raw data were collected from published public good experiments. We categorize studies by the number of periods (round lengths). Inclusion criteria: (1) standard linear public good game; (2) feedback on others' contributions after each round.

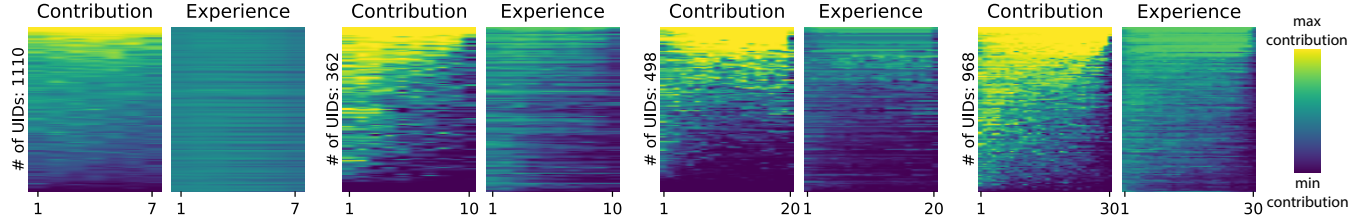


Figure S.1: Visualization of the Raw Data. The y-axis represents participant identifiers (UIDs), while the x-axis tracks the rounds played. Color intensity indicates the size of contributions, normalized between 0 and 1. The panels labeled 'Contribution' reflect each player's own contribution. The panels labeled 'Experience' represent the average contribution of the other players in the group during the preceding round. Within subplot-pairs, UIDs are sorted by their average contribution. Notably, there is heterogeneity with respect to the number of rounds played: The data is divided into subsets with games lasting 7, 10, 20, or 30 rounds. Furthermore, there exists heterogeneity concerning game parameters. Most notably, one study played a 7-round game (first column) with an exceptionally large group size of 100, resulting in unusually homogeneous average contributions.

E Details on the Clustering Analysis

E.1 Finding the Optimal Number of Clusters

To identify the appropriate number of behavioral clusters, we use three validity indices compatible with DTW-based clustering: the Silhouette Score [121], the Calinski–Harabasz Index [122], and Intra-cluster Variance [123]. Together, they evaluate cluster separation and the internal consistency of behavior. We compute each metric for $k = 2$ to $k = 20$, min–max normalize the results, and invert Intra-cluster Variance so that higher values consistently indicate better clustering. As shown in Fig. S.2, the average normalized score is highest for $k = 4$ –6, with a maximum at $k = 5$. Beyond $k = 6$, performance becomes unstable, and clusters shrink to sizes that limit interpretation. We therefore adopt $k = 6$ as a balanced solution—statistically strong while maintaining clear and interpretable behavioral groups. This approach aligns with recommendations that cluster validity indices serve as guidance rather than strict optimization rules [124].

Our dataset includes experiments with heterogeneous designs—different round lengths and group sizes—which shape behavioral dynamics. For example, the 7-round studies involve unusually large groups [125], the 20-round studies permit punishment and related enforcement-responsive strategies, and the 30-round studies resemble long-horizon interactions. By contrast, 10-round public goods games with 4-person groups represent the modal experimental design [90, 91]. To avoid overfitting to design-specific behavior, we use this standard subset to evaluate cluster validity and then apply the resulting six-cluster taxonomy across all studies. This ensures that our behavioral types reflect generalizable strategic patterns rather than experimental idiosyncrasies.

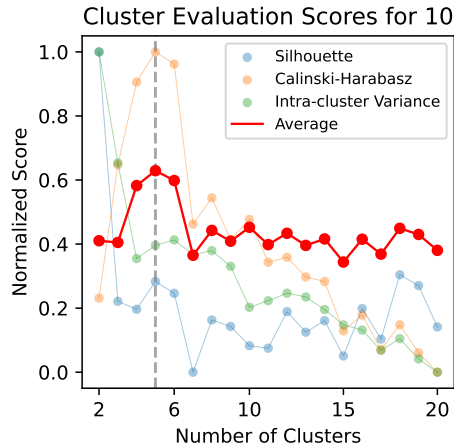


Figure S.2: Determining the Optimal Number of Clusters k . Normalized cluster evaluation scores (Silhouette, Davies–Bouldin, and Intra-cluster Variance) across different numbers of clusters. The vertical grey line indicates the selected solution with $k = 6$, which provides a trade-off between the evaluation metrics and maintains meaningful cluster sizes (each containing at least 30 members).

E.2 Assessing Cluster Stability and Heterogeneity

We evaluate cluster quality along two dimensions: (1) stability under resampling and (2) within-cluster heterogeneity. Stability assesses robustness to data perturbations, while heterogeneity tests whether clustering overfits by forcing all trajectories into six groups without a residual category.

We conduct non-parametric bootstrap resampling (100 replications, 80% subsample) to assess assignment robustness. Table S.3 reports subject-level stability, defined as the share of replications in which participants return to their baseline cluster. On average, participants return to their dominant cluster in 29.9% of replications ($SD = 3.3$ pp), well above the 16.7% expected under random assignment in a six-cluster design. Stability is similar across clusters (range: 27.2%–31.2%), suggesting that all clusters represent comparably robust behavioral patterns rather than noise. At the partition level, bootstrap solutions closely match the original clustering ($ARI = 0.861$, $SD = 0.061$; $NMI = 0.868$, $SD = 0.047$), confirming stable boundaries and assignments.

Despite this stability, substantial heterogeneity remains within clusters. We quantify heterogeneity using silhouette scores, which range from -1 (closer to another cluster) to $+1$ (strong fit to the assigned cluster). As shown in Table S.4, cluster coherence varies widely: Clusters 1 and 6 exhibit strong internal structure (mean silhouette > 0.46), while Clusters 2 and 4 show weak separation (mean silhouette < 0.05). Furthermore, 26.9% of participants have negative silhouette scores, meaning their trajectories are closer (on average) to another cluster than to the one they are assigned. Distance-based metrics tell a similar story. The average distance between trajectories within the same cluster is 1.87 ($SD = 0.49$), while the average distance between trajectories in different clusters is only modestly larger at 2.92 ($SD = 1.00$). Consistent with this overlap, a DTW-based variance decomposition partitions total trajectory dispersion into between- and within-cluster components. Clusters account for 29.5% of total variance—reflecting differences between cluster-average trajectories—while the remaining 70.5% reflects variation among individuals within the same cluster.

Thus, clusters summarize dominant behavioral patterns while leaving substantial individual-level variation unexplained. This is consistent with extensive evidence from the PGG literature that individual contribution paths exhibit considerable idiosyncratic variation. The fact that clusters are stable across resampling yet retain substantial within-cluster heterogeneity indicates that they capture systematic tendencies without artificially suppressing behavioral noise.

Table S.3: Subject-Level Cluster Stability

	Cl. 1	Cl. 2	Cl. 3	Cl. 4	Cl. 5	Cl. 6	Overall
Mean Stability (%)	30.5	31.2	29.2	31.2	30.1	27.2	29.9
SD (pp)	3.7	2.0	3.1	3.8	3.2	2.9	3.3

Note: Mean stability indicates the share of bootstrap replications (100 replications, 80% subsample) in which subjects return to their baseline cluster. SD reflects variability across subjects within each cluster (percentage points, pp). Random assignment benchmark: 16.7%.

Table S.4: Within-Cluster Heterogeneity and Fit Quality

	Cl. 1	Cl. 2	Cl. 3	Cl. 4	Cl. 5	Cl. 6	Overall
Mean Silhouette	0.47	0.00	0.10	0.05	0.29	0.48	0.13
SD	0.08	0.13	0.11	0.15	0.11	0.08	0.21

Note: Silhouette scores range from -1 to $+1$; negative values indicate participants closer to an alternative cluster. Within-cluster distance: $M = 1.87$ ($SD = 0.49$); between-cluster distance: $M = 2.92$ ($SD = 1.00$); separation ratio: 1.56. Overall, 26.9% have negative silhouette scores.

E.3 Effect of Distance Metrics on Clustering Results

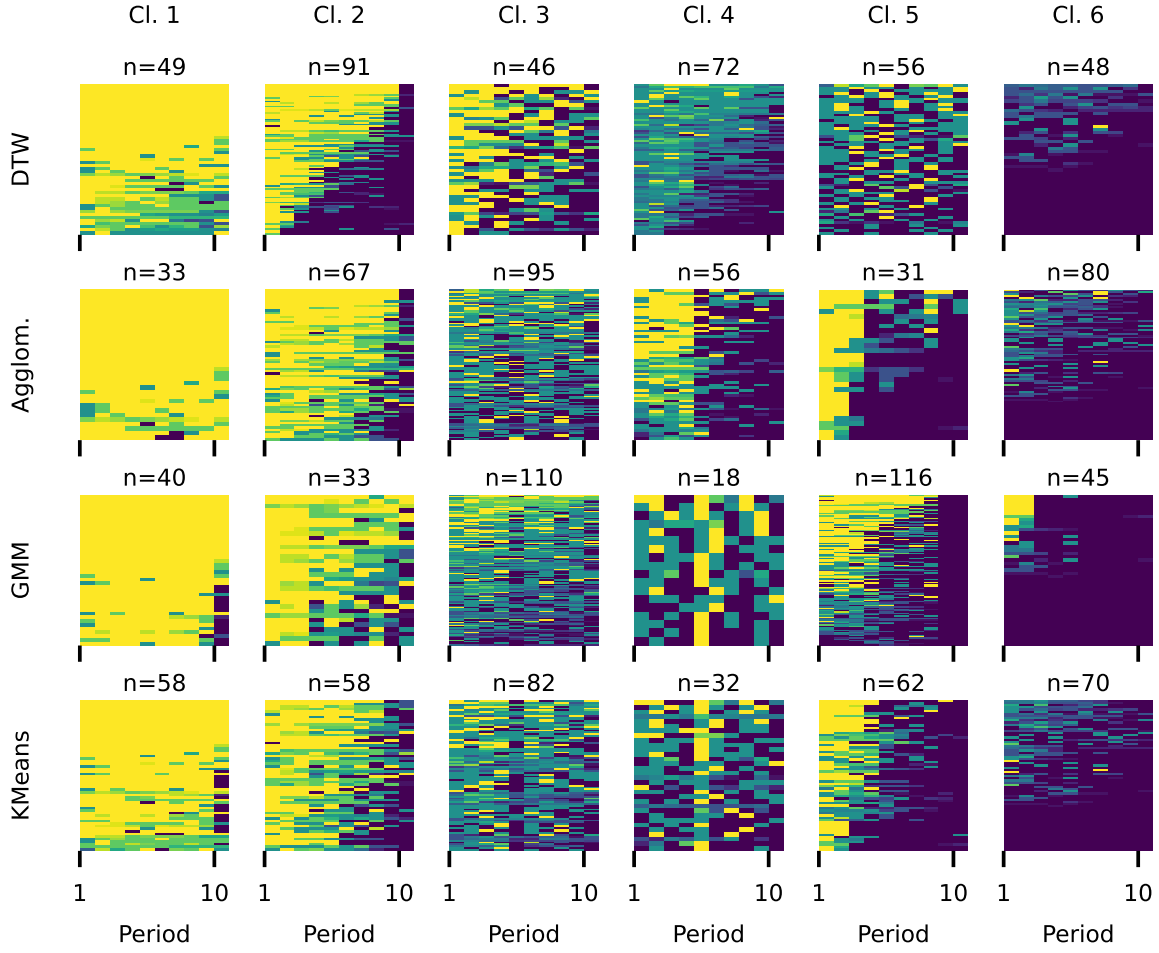


Figure S.3: Comparison of Distance Metrics. Clustering based on DTW k-means (top row) is contrasted with Euclidean-based clustering (bottom row), including agglomerative clustering, Gaussian mixture models and k-means. Euclidean distance enforces strict pointwise alignment across rounds, producing vertically aligned contribution patterns. A behavioral profile defined by a sharp drop from high to very low contributions is consistently detected across methods but may be assigned to different clusters under Euclidean agglomerative clustering.

We illustrate that the choice of distance metric makes a qualitative difference in the clustering outcomes. Euclidean distance allows only for local alignment, whereas DTW enables global alignment—meaning that time series exhibiting the same overall pattern but shifted in time can be grouped into the same cluster. We generate a comprehensive grid of comparisons: DTW paired with k-means, Euclidean distance paired with k-means, Gaussian Mixture Models (GMM), and agglomerative clustering.

Fig. S.3 shows that all Euclidean-based results display vertically aligned contribution patterns.

For illustrative purposes, we focus on the cluster type characterized by a sharp transition from very high to very low contributions. This cluster (Cluster 2 under DTW) is most clearly visible among the Euclidean-based clusters in the agglomerative (row 2) outcomes. We therefore select these two methods—DTW with k-means and Euclidean with agglomerative clustering—for direct comparison in the main text (Fig. 2).

We further analyze the threshold-switching hypothesis. Cluster 2 in the DTW results suggests the existence of a behavioral type that switches from very high to very low contributions quite abruptly, and that this switch can occur at any point in time. An alternative hypothesis is that switching occurs only at specific, time-locked points in the game. To test these hypotheses, we identify, for each participant, the round in which the most dramatic change in contributions occurs. We then group participants based on these switching points (Fig. S.4). Clusters 1 and 9

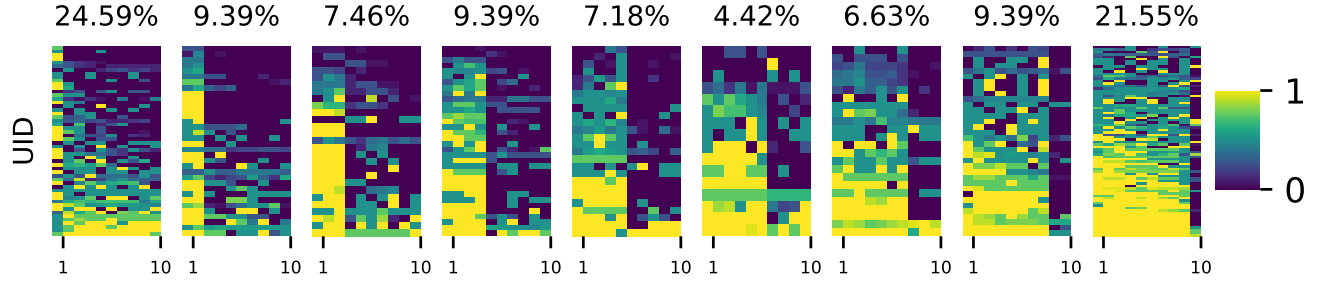


Figure S.4: Distribution of Optimal Threshold Points Across Rounds. Each subplot represents the percentage of players who showed their most dramatic change in contribution level at that round. Heatmaps of contributions are shown, subsetted by the round in which the switching process occurs.

together contain nearly 50% of participants and are visually the least distinct, while the remaining clusters each include between 4.4% and 9.4% of participants. Notably, Clusters 1 and 9 do not display the strong yellow–dark blue contrast that characterizes the sharp “high-to-low” transition observed in Cluster 2 (DTW). While the relative size of these clusters is indeed higher than that of the others, the absence of a clear color transition indicates that they do not capture the same extreme switching behavior. Across the remaining clusters, each cluster has a nonzero share of participants, suggesting that switching can occur at any round. Overall, this analysis supports the interpretation that extreme switching behavior is not tied to a specific point in time but can arise idiosyncratically at any stage of the game.

E.4 Comparison of Clustering Algorithms

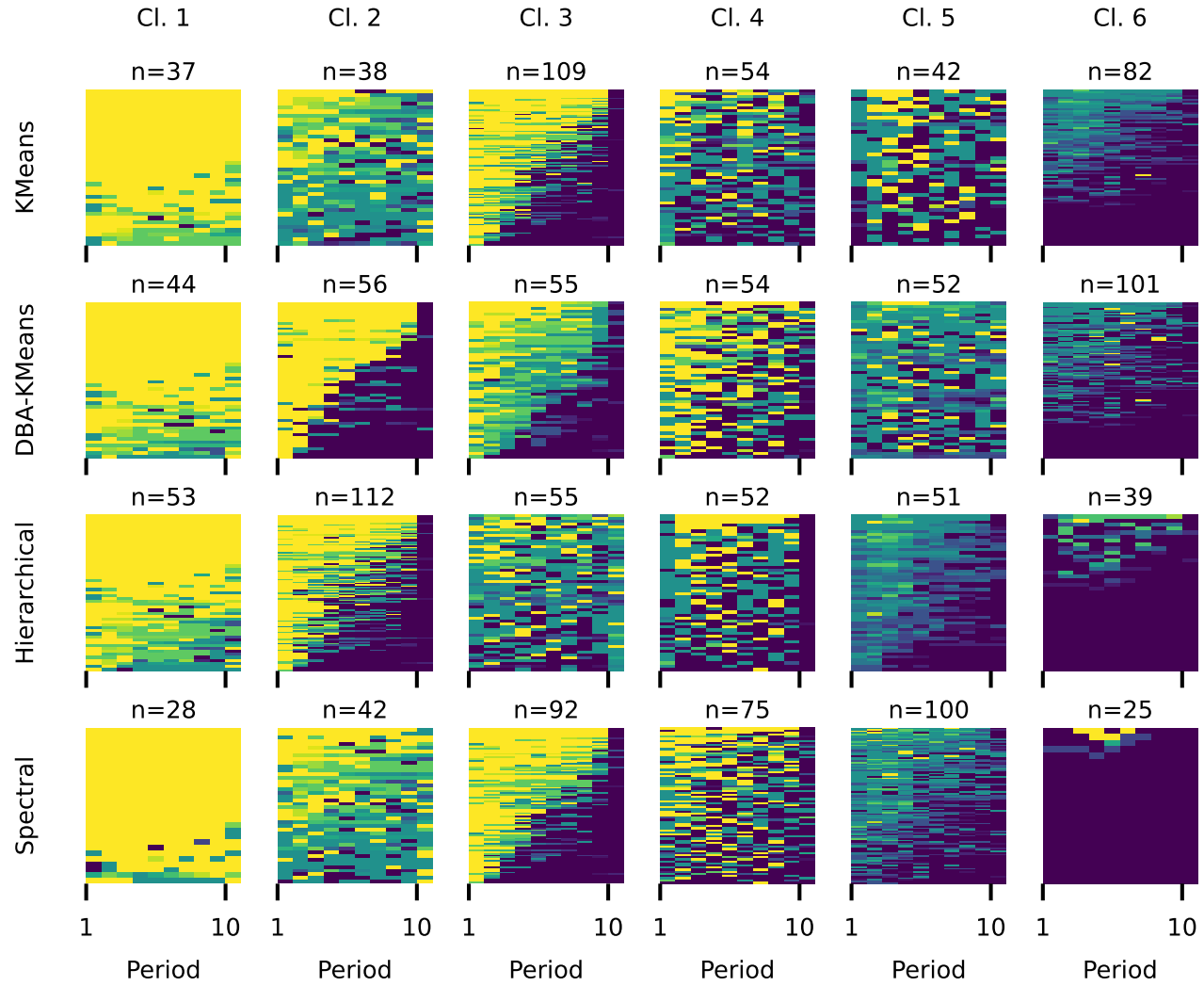


Figure S.5: Comparison of Clustering Algorithms in Combination with DTW. We examine combinations of DTW with K-means, hierarchical clustering, and spectral clustering. For this analysis, the number of clusters is fixed to six, focusing on the data subset with 10 rounds. The results indicate that spectral clustering most distinctly separates the data.

Having identified DTW as the most suitable distance metric for our data, we evaluated its performance in combination with four clustering algorithms: K-means, DBA K-means, hierarchical clustering, and spectral clustering (see Fig. S.5). Overall, the resulting clusters are highly similar across all algorithms, indicating that the underlying structure of the data is stable and can be reliably identified by different methods when the appropriate distance metric is applied.

Qualitatively, spectral clustering produced the most clearly distinct *freeriding* cluster as well as the most pronounced *unconditional contribution* cluster. Therefore, we selected spectral clustering for all subsequent analyses.

E.5 Comparison of Partitioning Methods from the Literature

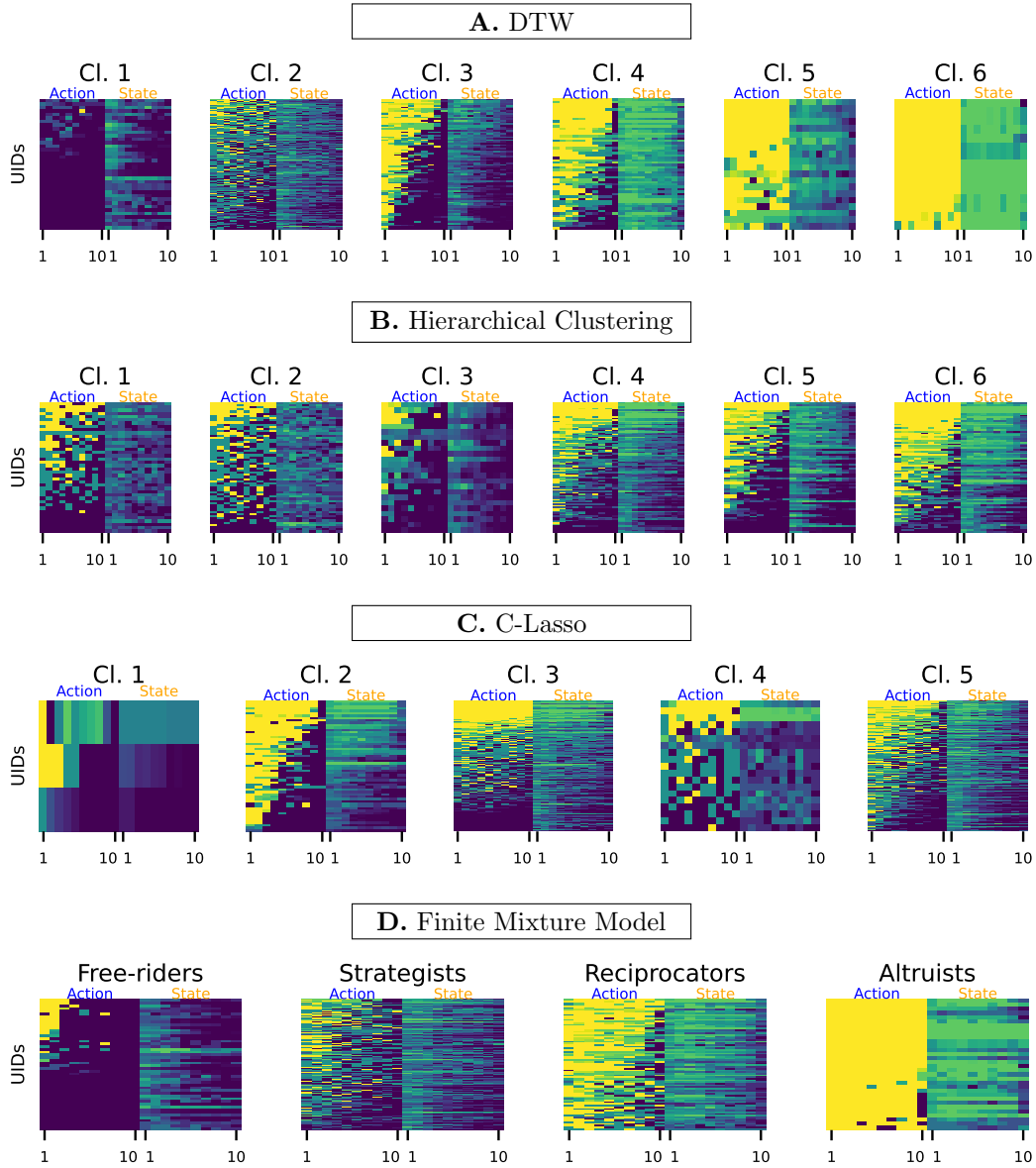


Figure S.6: Comparison of partitioning methods. (A) Dynamic Time Warping (DTW) and Spectral Clustering, (B) Hierarchical Clustering [39], (C) Classifier-Lasso [47], and (D) Finite Mixture Models [43]. We argue that DTW provides the sharpest separation of temporal patterns in our panel data.

Each method tested in Fig. S.6 produces a distinct partition of the participant trajectories.

The finite mixture model is predefined to identify four behavioral types: freerider, altruist, reciprocator, and strategist. While the freerider and altruist clusters are clearly delineated, the reciprocator and strategist clusters are relatively large and noisy.

C-Lasso converged with five clusters rather than our proposed six. Its first cluster contains only three participants, whereas the others are comparatively large. Interestingly, Cluster 2 and Cluster 5 show similar temporal patterns. However, Cluster 3 mixes unconditional cooperators with consistent freeriders.

Hierarchical clustering produced six clusters but failed to recover the most prominent and interpretable types, namely the altruist and freerider groups.

By contrast, our DTW + Spectral Clustering approach generates clusters that are both temporally aligned and behaviorally coherent.

F Full Sample Plots

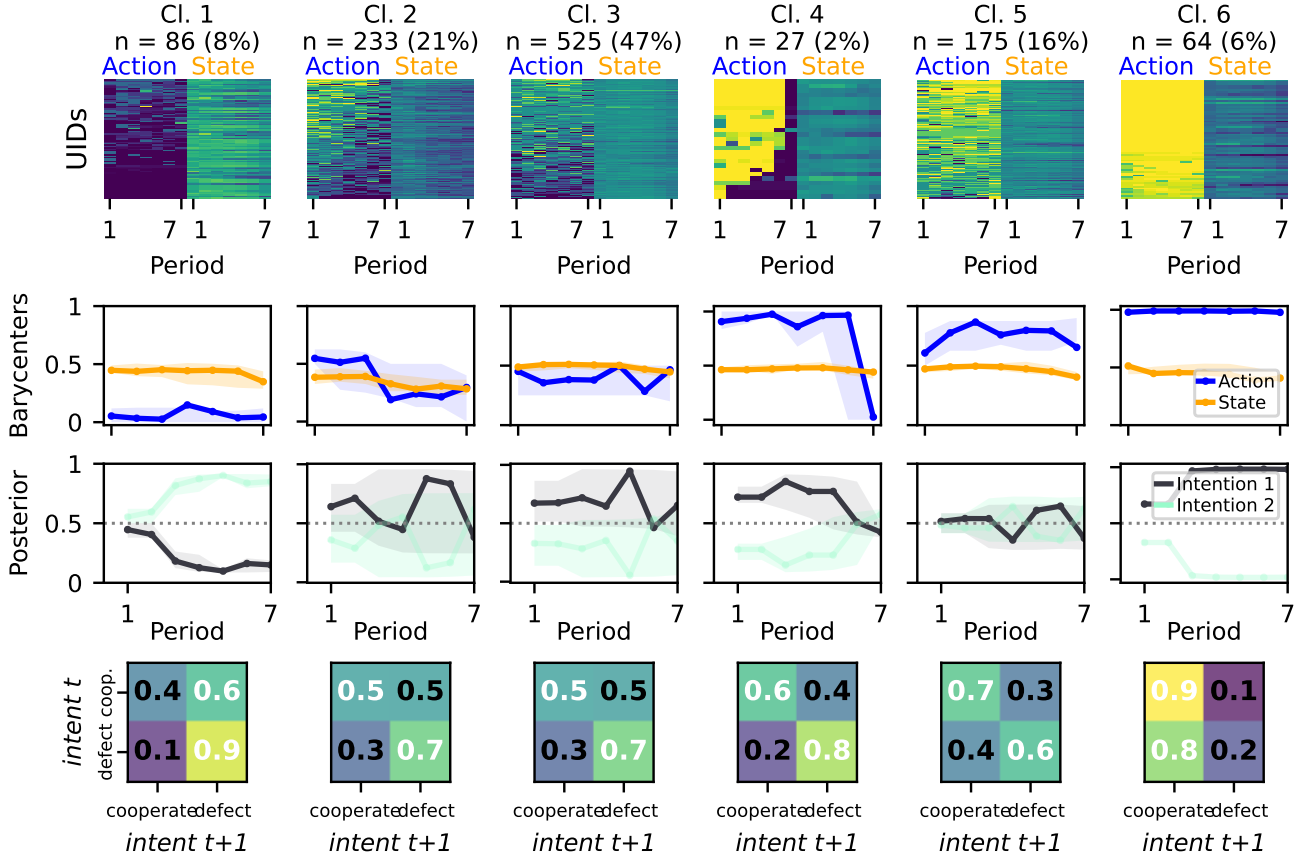


Figure S.7: Clustering Analysis of Action-State Patterns and Intention Dynamics. (1) Heatmaps of action and state trajectories per cluster, ordered by mean action. (2) DTW barycenters of action-state patterns per cluster, with interquartile ranges shaded. (3) DTW barycenter averages of posterior intentions per cluster, with interquartile ranges shaded. (4) Average transition probabilities between cooperative and defecting intentions per cluster.

Our dataset includes experimental games with varying lengths of play: 7, 10, 20, and 30 rounds. Each subset exhibits distinct structural and behavioral characteristics. The 7-round subset is unique in that group sizes were exceptionally large—sometimes including up to 100 participants—which tends to stabilize average experiences across rounds. As a result, the state heatmaps appear markedly more uniform in this subset than in any of the others. The 20-round subset differs in another important respect: it includes a punishment treatment. This feature likely explains the distinctive pattern observed for Cluster 3 in this condition (row 3), where contributions start low (dark purple) but subsequently rise to high levels (yellow)—a dynamic not seen in any other subset.

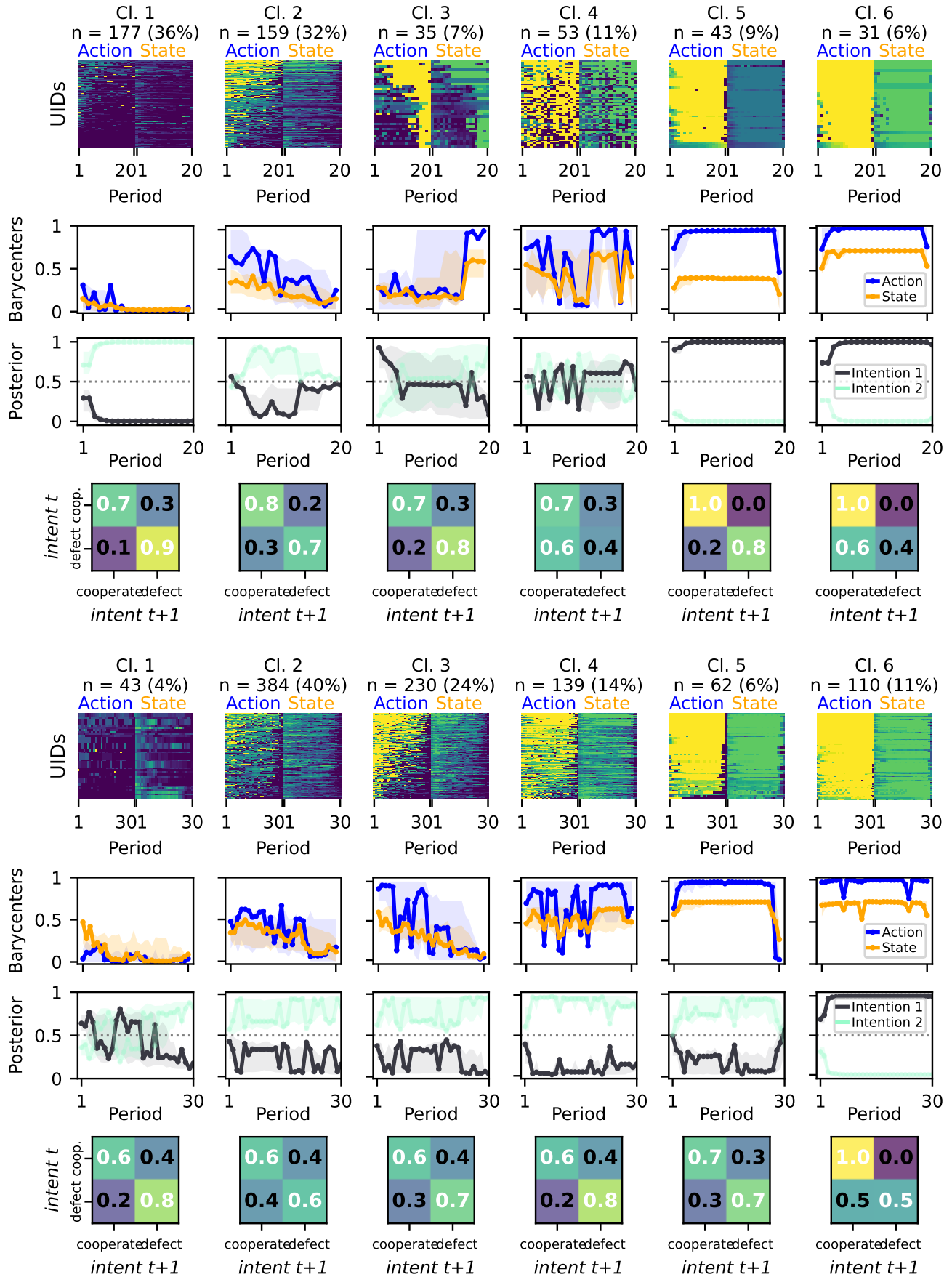


Figure S.8: Clustering Analysis of Action-State Patterns and Intention Dynamics. Additional panels for round lengths 20 and 30.

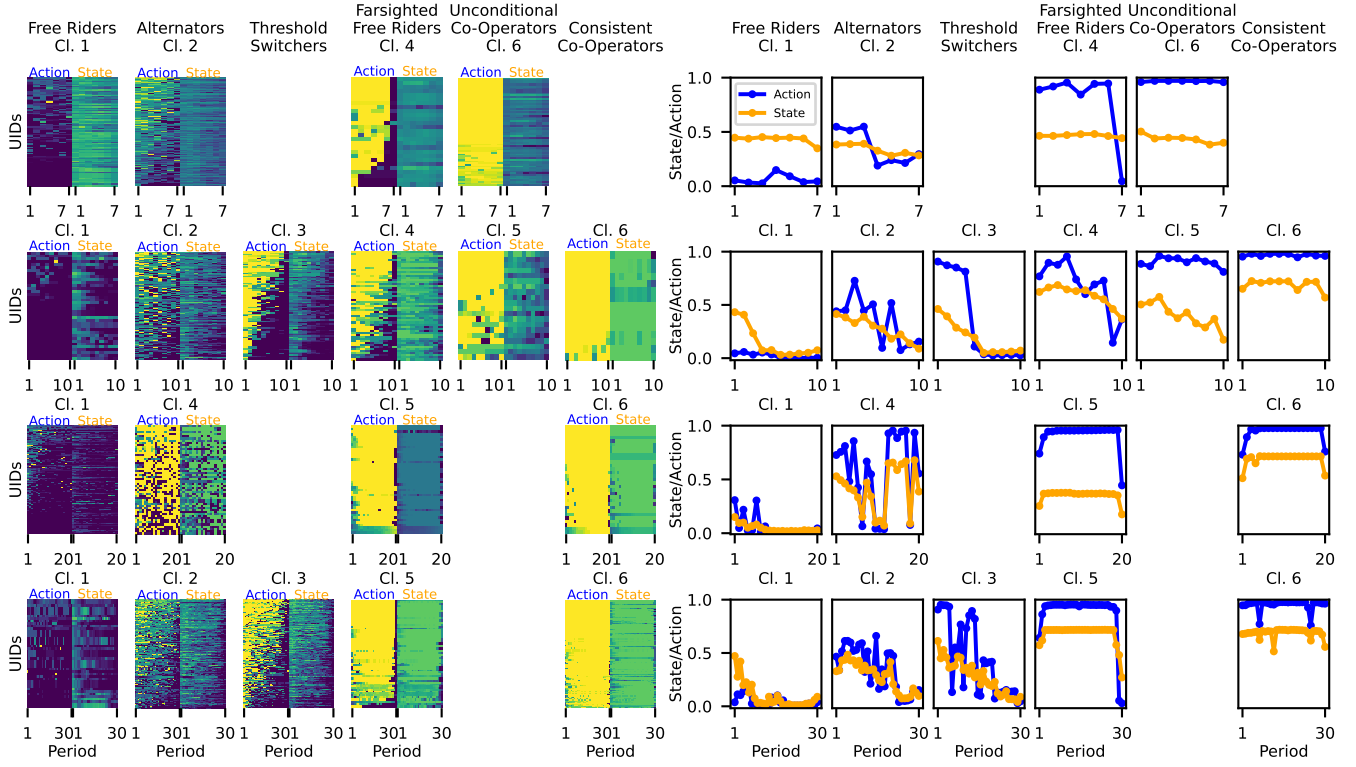


Figure S.9: Behavioral Types Across Game Lengths. The figure displays behavioral clustering results across four game lengths (7, 10, 20, and 30 periods). Each column represents a distinct behavioral type: Free Riders, Alternators, Threshold Switchers, Farsighted Free Riders, Unconditional Co-Operators, and Consistent Co-Operators. For each type, the left panel shows individual contribution patterns as heatmaps (with action and state contributions side-by-side), while the right panel displays the DBA-computed barycenter trajectories of actions and states over time. Rows correspond to different game lengths. Empty cells indicate that a particular type was not identified in that subset.

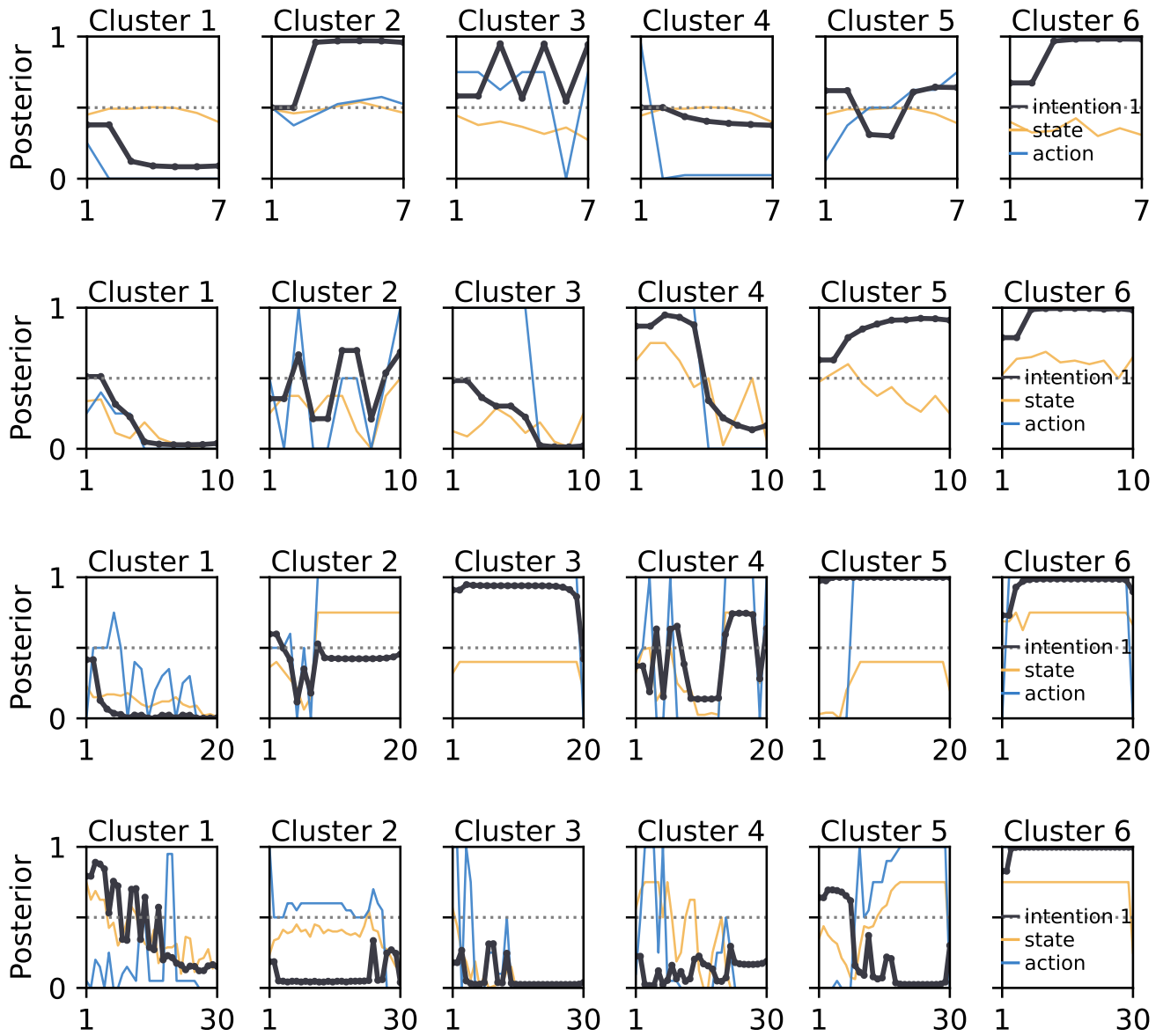


Figure S.10: Sampled UIDs with Actions, States and Fitted Intention-Dynamics from Each Cluster. Illustration of how observed actions and states inform latent intention adoption. For each cluster, we display randomly selected individuals and plot three aligned time series: their contributions (actions), their inferred states, and the posterior probability of adopting Intention 1. Because the model is based on two intentions, the probability of Intention 2 is simply one minus the plotted value.

G Number of Latents and Log Likelihoods

Table S.5: Optimal Number of Latent Intentions: $K = 2$.

Transition (K)	Δ Test LL	Δ BIC
$1 \rightarrow 2$	0.66	75.2
$2 \rightarrow 3$	0.31	88.7
$3 \rightarrow 4$	0.19	101.6
$4 \rightarrow 5$	0.19	114.4

Note: Model comparison based on changes in test log-likelihood and Bayesian Information Criterion (BIC) when increasing the number of latent intentions (K). The transition from one to two intentions yields the largest improvement in test log-likelihood and the smallest rise in BIC, indicating that a two-intention model provides the best fit to the data.

H Model Performance per Cluster and Subset

Table S.6: Model Performance per Cluster and Subset.

	Subset 7	Subset 10	Subset 20	Subset 30
Cluster 1	-0.22 ± 0.04	-0.24 ± 0.03	-0.29 ± 0.02	-0.38 ± 0.01
Cluster 2	-0.75 ± 0.02	-0.72 ± 0.02	-0.46 ± 0.06	-0.81 ± 0.01
Cluster 3	-0.82 ± 0.02	-0.59 ± 0.03	-0.71 ± 0.02	-0.74 ± 0.02
Cluster 4	-0.75 ± 0.11	-0.88 ± 0.08	-0.44 ± 0.04	-0.53 ± 0.03
Cluster 5	-0.69 ± 0.02	-0.67 ± 0.24	-0.33 ± 0.06	-0.61 ± 0.02
Cluster 6	-0.21 ± 0.06	-0.33 ± 0.21	-0.18 ± 0.05	-0.12 ± 0.01

Note: The model was fit across five cross-validation folds and ten repetitions. To assess model performance comprehensively, test log-likelihoods were first averaged across folds and repeats for each participant, and these participant-level means were then aggregated within each cluster. As the values represent log-likelihoods, less negative values indicate a better model fit to the human behavioral data.

In IRL models, log-likelihood (LL) is used as a standard metric of model fit because it directly quantifies how probable the observed choices are under the fitted model—higher (less negative) values indicate that the model assigns greater probability to the actual behavior observed. However, it is important to note that LL not only measures model performance but also reflects the inherent noise in the behavioral data being modeled. Table S.6 shows differences in model fit across clusters. These differences in log-likelihoods capture underlying variation in behavioral noisiness. IRL models explain observed actions by assuming they arise from approximately optimal reward-driven behavior; therefore, the attainable log-likelihood depends on how consistent participants’ actions are with such a structure.

When participants behave deterministically or follow stable strategies—as in Cluster 1 (-0.24 ± 0.03) and Cluster 6 (-0.33 ± 0.21)—the model can closely reproduce their choices, yielding high (less negative) log-likelihoods. Conversely, when behavior is highly stochastic—such as in Cluster 2 (-0.72 ± 0.02), where participants alternate unpredictably between extreme actions—the data contain more “decision noise,” and even the best-fitting model achieves lower likelihood. Hence, the fitted log-likelihood serves as an empirical indicator of behavioral noisiness: the more random the observed actions, the poorer the attainable fit [for more details see 126, p.9].

I Additional Analyses

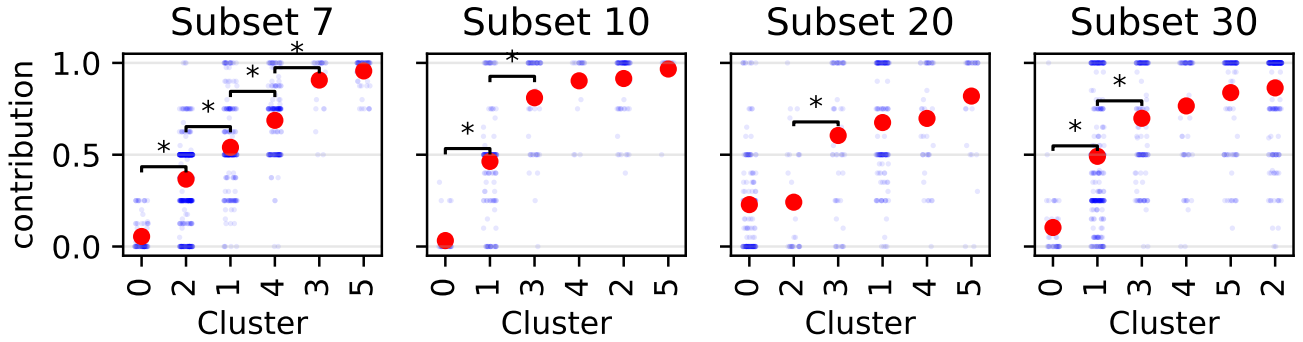


Figure S.11: First Round Contributions by Cluster. Each panel shows data from one subset size (7, 10, 20, or 30 participants). Within each subset, clusters are ordered along the x-axis according to their mean normalized contribution during the first round. Blue points represent individual participant contributions, and red circles indicate the mean contribution for each cluster. Adjacent clusters were compared using Welch's two-sample t-tests; black brackets mark pairs of neighboring clusters whose means differ significantly ($p < 0.05$).

First-round contributions are widely viewed as informative about underlying social preferences and early learning. Some work argues that these contributions matter chiefly in the initial round, when social motives are most salient, whereas later behavior is dominated by payoff-based learning. Motivated by this, we examined unconditional first-round contributions and the average contribution of group members by cluster (Fig. S.11). We tested for differences across clusters using Welch's two-sample t-tests. Not all clusters differ significantly on either measure. Thus, initial contributions alone do not determine cluster membership; instead, clustering appears to reflect how individuals experience the interaction and adapt to those experiences, beyond their initial choices.